SURVEY AND SUMMARY

Single-molecule imaging of epigenetic complexes in living cells: insights from studies on Polycomb group proteins

Kyle Brown, Haralambos Andrianakos, Steven Ingersoll and Xiaojun Ren [ID]*

Department of Chemistry, University of Colorado Denver, Denver, CO 80217-3364, USA

ABSTRACT

Chromatin-associated factors must locate, bind to, and assemble on specific chromatin regions to execute chromatin-templated functions. These dynamic processes are essential for understanding how chromatin achieves regulation, but direct quantification in living mammalian cells remains challenging. Over the last few years, live-cell single-molecule tracking (SMT) has emerged as a new way to observe trajectories of individual chromatin-associated factors in living mammalian cells, providing new perspectives on chromatin-templated activities. Here, we discuss the relative merits of live-cell SMT techniques currently in use. We provide new insights into how Polycomb group (PcG) proteins, master regulators of development and cell differentiation, decipher genetic and epigenetic information to achieve binding stability and highlight that Polycomb condensates facilitate target-search efficiency. We provide perspectives on liquid-liquid phase separation in organizing Polycomb targets. We suggest that epigenetic complexes integrate genetic and epigenetic information for target binding and localization and achieve target-search efficiency through nuclear organization.

INTRODUCTION

Eukaryotic DNA is wrapped around histones to form nucleosomes and chromatin, which dictates accessibility of underlying DNA for chromatin-associated proteins (1,2). Such selective access to specific chromatin regions by chromatin-associated factors allows for exertion of specific chromatin-templated functions, which instructs metabolism of nucleic acids. Because of this, how chromatin-associated factors locate, bind to, and assemble on specific chromatin regions has been the target of decades of theoretical discussions and experimental studies (3–6). Additionally, chromatin is organized at a variety of scales, from chromosome territories (hundreds of megabases) down to individual nucleosomes (147 base pairs) with intermediate sized topologically associating domains (TADs, kilobase to megabase) that show high rates of intra-TAD interaction relative to inter-TAD interaction (7–9). Furthermore, chromatin-associated factors often self-organize to form compartments/condensates in the nucleus (10). Emerging data imply that the interplay between dynamics and compartmentalization of chromatin-bound factors and genome organization orchestrates chromatin-templated functions (9).

Polycomb group (PcG) proteins are a paradigm that has been utilized to understand how chromatin-associated proteins regulate gene transcription (11–13). PcG proteins are evolutionarily conserved master regulators of development, and mutation and dysregulation of PcG genes often cause developmental defects and/or cancer (14). PcG proteins have been genetically and biochemically divided into two histone-modifying complexes, Polycomb repressive complex (PRC) 1 and 2 (11–14) (Figure 1). PRC2 is a methyltransferase that methylates histone H3 on lysine 27 (H3K27me1/me2/me3) (15–19). H3K27me3 provides a binding site for PRC1 (20). PRC1 is a ubiquitin ligase that ubiquitinates histone H2A at lysine 119 (H2AK119Ub1) (21,22), which impacts PRC2 recruitment (23–25). Thus, PRC1 and PRC2 form a feedback loop to reinforce each other's activity in establishing and maintaining transcription programs. Studies have shown that both PRC2 and PRC1 are involved in establishing long-range chromatin interactions (26–31). Consistently, recent studies demonstrate that PRC1 phase separates to assemble Polycomb conden-
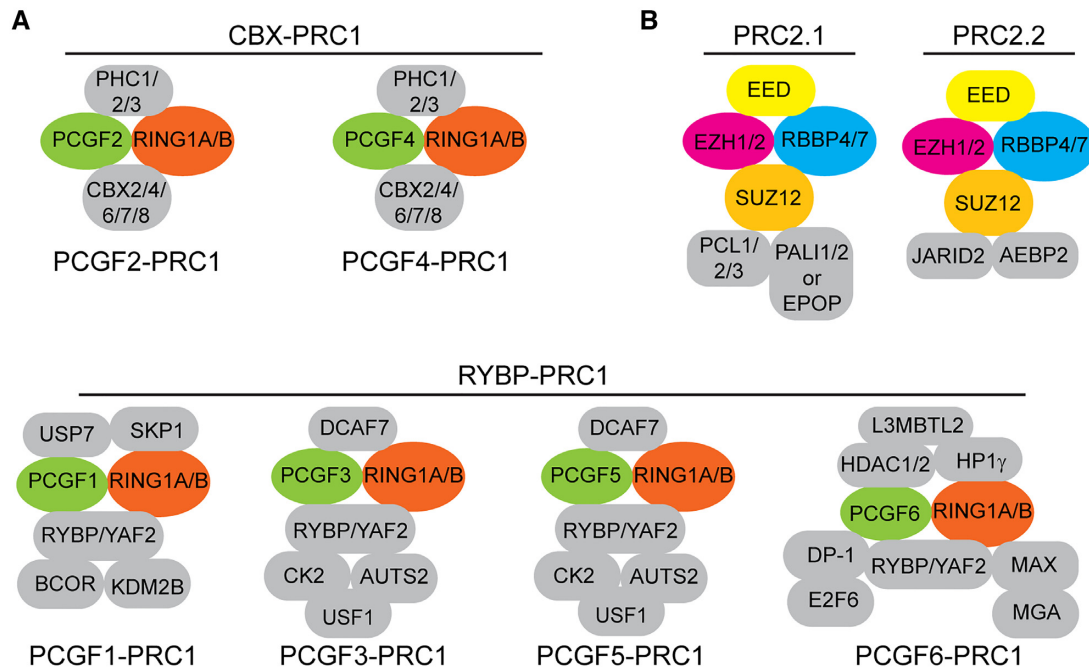
Figure 1. Schematic description of the two major PcG complexes. (**A**) Two major classes of PRC1 complexes: CBX-PRC1 and RYBP-PRC1. The PRC1 complexes assemble around the catalytic core, one copy of the six PCGF1–6 paralogs and one of the E3 ubiquitin ligase RING1A/B. They are divided into canonical PRC1 (CBX-PRC1) or variant PRC1 (RYBP-PRC1). The CBX-PRC1 complexes contain the RING1A/B-PCGF2/4 core, one copy of the CBX2/4/6/7/8 paralogs, and one copy of the PHC1–3 subunits, giving rise to the two canonical PCGF2- and PCGF4-PRC1 complexes, respectively. The RYBP-PRC1 complexes contain RYBP/YAF2 instead of one of the CBX proteins. RYBP and YAF2 are able to recognize the H2AK119Ub1 mark, which promotes RYBP-PRC1 ubiquitin ligase activity. The catalytic core is colored and additional subunits are gray. (**B**) Two major classes of PRC2 complexes: PRC2.1 and PRC2.2. The minimally catalytic core of PRC2 is comprised of one copy of EZH1/2, EED and SUZ12. The core stoichiometric PRC2 complex consists of the catalytic core and one copy of RBBP4/7. The PRC2 complexes are divided into two major subcomplexes, PRC2.1 and PRC2.2. PRC2.1 contains one copy of PCL paralogs (PCL1/PHF1, PCL2/MTF2 or PCL3/PHF19) and one of two auxiliary proteins, EPOP or PALI1. PRC2.2 contains the JARID2 and AEBP2 auxiliary proteins. These auxiliary proteins within PRC2.1 and PRC2.2 cooperate to deposit H3K27me3 *via* synergetic and independent mechanisms. The catalytic core is colored and auxiliary proteins are gray.

sates (32–35), which function as compartments for repressing Polycomb target genes (27,35–41).

Within the last few decades, numerous biochemical and genetic studies have been performed to dissect how PcG proteins locate and bind their cognate sites to establish chromatin microenvironments that facilitate repressive states of Polycomb target genes (11–14). Classical biochemical and biophysical studies have proposed a series of mechanisms concerning how PcG proteins locate and bind to chromatin. However, these mechanisms cannot fully explain observations from genetic perturbations, which is, in part, due to the fact that biochemical and biophysical experiments cannot completely recapitulate cellular environments. Chromatin immunoprecipitation coupled with next-generation sequencing (ChIP-seq) and genetic perturbations have been widely used to examine binding mechanisms of PcG proteins, which has provided significant insights into the mechanisms that enable PcG proteins to bind chromatin. Nonetheless, ChIP-seq is based on cross-linking chemistry whose efficiency is determined by multiple factors, including, but not limited to, structural orientation, molecular stoichiometry, and molecular abundance, which confounds analysis of binding mechanisms. Moreover, the cross-linking of protein-DNA by formaldehyde is ineffective when their interaction time is below ∼5.0 s (42,43),

which falls into residence-time scale of some transcription regulatory factors (43–54). Thus, it is difficult to establish a quantitative model that predicts and describes how PcG complexes locate, bind to, and assemble on target sites with this methodology.

Recent advances in microscopy and fluorophores enable direct visualization of chromatin-associated complex trajectories in the nucleus of mammalian cells. Thus, how chromatin-associated complexes search for, associate with, and assemble on chromatin can be quantitatively measured (5,6). In combination with genetic manipulation, the molecular mechanism underlying the dynamics of chromatin-associated factors in metabolism of nucleic acids can be dissected and the impact of nuclear compartments and chromatin organization on transcriptional dynamics can be assessed. Here, we summarize recent applications of live-cell single molecule tracking (SMT) in the Polycomb field and highlight new molecular insights revealed by live-cell SMT. We provide perspectives in the further development of live-cell SMT to answer outstanding questions in the epigenetic field. This Survey and Summary focuses on the application of live-cell SMT to PcG complexes. For other applications of live-cell SMT, such as transcription factors in mammalian cells and prokaryotic cells, please refer to other excellent reviews (5,6,55–60).

POLYCOMB REPRESSIVE COMPLEXES

Polycomb repressive complex 2

The minimal catalytic core of PRC2 that enables methylation of all histone H3 is composed of one copy of EZH1/2, EED and SUZ12 (61,62) (Figure 1B). The stoichiometric PRC2 complex consists of the catalytic core and one copy of RBBP4/7 (61,62). EZH1/2 are the catalytic subunits of PRC2 methyltransferase (15–19). EZH2-PRC2 has stronger methyltransferase activity than EZH1-PRC2 (19,63). EED binds H3K27me3, which allosterically stimulates PRC2 methyltransferase activity (64,65). SUZ12 mediates PRC2 recruitment (66–68). RBBP4/7 are histone-binding proteins (69). The PRC2 core complex assembles into two distinct subcomplexes, PRC2.1 and PRC2.2, by interacting with several substoichiometric components that regulate its enzymatic activity or recruitment (61,62). PRC2.1 contains one copy of PCL paralogs (PCL1/PHF1, PCL2/MTF2 or PCL3/PHF19) and one of two auxiliary proteins, EPOP or PALI1 (70–72). PCL proteins recognize H3K36me2/3, an activating mark, which stimulates PRC2 methyltransferase activity (73–76). PHF1 and MTF2 bind CG-rich DNA to promote PRC2 association with chromatin (77,78). EPOP binds to Elongin B/C proteins and promotes PRC2 methyltransferase activity *in vitro* (70,72,79). PALI1 also promotes PRC2 activity *in vitro* (71). PRC2.2 contains the JARID2 and AEBP2 auxiliary proteins (61,62). Both JARID2 and AEBP2 preferentially bind CG-rich DNA, which is thought to recruit PRC2 to chromatin (80–82). Additionally, they also bind H2AK119Ub1 deposited by PRC1, which promotes PRC2 methyltransferase activity (23–25,83,84). These auxiliary proteins within PRC2.1 and PRC2.2 cooperate to deposit H3K27me3 *via* synergistic and independent mechanisms (68,85,86).

Polycomb repressive complex 1

The PRC1 complexes are more diverse than PRC2. The catalytic core components of PRC1 are one of the six PCGF1–6 paralogs and one of RING1A/B (12,13) (Figure 1A). RING1A/B are the E3 ubiquitin ligases that catalyze monoubiquitination of H2AK119 (21,22). Six PRC1 subcomplexes have been identified, which are characterized by the incorporation of specific PCGF isoforms and other accessory proteins and can be classified as CBX-PRC1 and RYBP-PRC1 (87–90). PCGF2/4 can also interact with RYBP and YAF2 to form trimeric RYBP/YAF-PCGF2/4-RING1A/B complexes (88,89), which have more active ubiquitination ligase activity than CBX-PRC1 (88).

The CBX-PRC1 complexes assemble around the RING1A/B-PCGF2/4 core and contain one copy of the CBX2/4/6/7/8 paralogs and one copy of the PHC1–3 subunits, giving rise to the two canonical PRC1.2 and PRC1.4 complexes, respectively (87,89). PCGF2/4 are also known as MEL18 and BMI1, respectively. The CBX proteins contain characteristic chromodomains with varying affinities for H3K27me3 (91–93) and are thought to play a key role in recruiting CBX-PRC1 to target sites. The PHC proteins contain a sterile alpha motif (SAM) domain that can self- or hetero-polymerize, which is essential for PcG-mediated repression (27,94). The CBX-PRC1 complexes are involved in establishing long-range chromatin interactions that lead to chromatin compaction (26–30). The activity behind CBX-PRC1 compacting chromatin has been determined to be from CBX2 (95,96). Mutating CBX2 residues that are required for compaction leads to homeotic transformations that are similar to those observed in PcG loss-of-function mutations (96). Both CBX2 and the SAM domain of *Drosophila* Ph can undergo liquid-liquid phase separation to form condensates (32–35). These condensates function as compartments for Polycomb target gene repression (27,35–41).

The RYBP-PRC1 complexes contain RYBP or its YAF2 paralog, both of which compete with CBX for the same binding pocket on the C-terminal domain of RING1B (87,88,97,98). The RYBP-PRC1 complexes are more active H2AK119 ubiquitin ligases than the CBX-PRC1 complexes (99–102). PCGF1-PRC1 contains KDM2B, which recognizes CG-rich DNA (103–105), promoting its recruitment to target sites. PCGF6-PRC1 associates with MGA/MAX/DP-1/MGA DNA-binding factors, which targets the complex to a subset of development-related genes (100,106,107). PCGF3 interacts with the transcription factor USF1, which targets the PCGF3-PRC1 complex to specific chromatin regions (100). The RYBP-PRC1-deposited H2AK119Ub1 is central for repressing Polycomb target genes (100,101,108,109).

LIVE-CELL SINGLE-MOLECULE TRACKING

Live-cell SMT requires labelling of chromatin-associated factors within cells as well as a sensitive imaging set up capable of detecting individual complexes within the crowded, complex nucleus (Figure 2A).

Generation of fusion protein in living cells

Labelling for a single-molecule experiment is different from traditional cellular imaging in that only a subset of the molecular population should be visible to allow for precise identification of individual molecules, typically below 15 molecules in any given frame within the nucleus, or approximately <0.5 molecules per squared micrometer within the nucleus. This is generally achieved by genetically fusing the protein of interest with photoswitchable fluorescent proteins or self-labeling enzyme tags such as HaloTag (HT) (43,45,48,51,110). By controlling laser power and illumination time, a subset of photoswitchable fluorescent proteins can be turned on from dark states to fluorescent states, allowing individual chromatin-associated complexes to be visualized (51). While photoswitchable fluorescent proteins revolutionized imaging techniques, particularly in super-resolution imaging, they are not adequately photostable and lack a high quantum yield (111). This prevents long-term observation of trajectories of epigenetic complexes, which is crucial for residence time measurement by live-cell SMT. Self-labelling enzyme tags use organic ligands, such as Janelia Fluorescent (JF) dyes or photoactivatable dyes, such as PA-JF dyes, which have greater photostability and quantum efficiency than fluorescent proteins (111,112), allowing for dynamics of a variety of epigenetic factors to be explored. By sparse labelling of tagged proteins using low
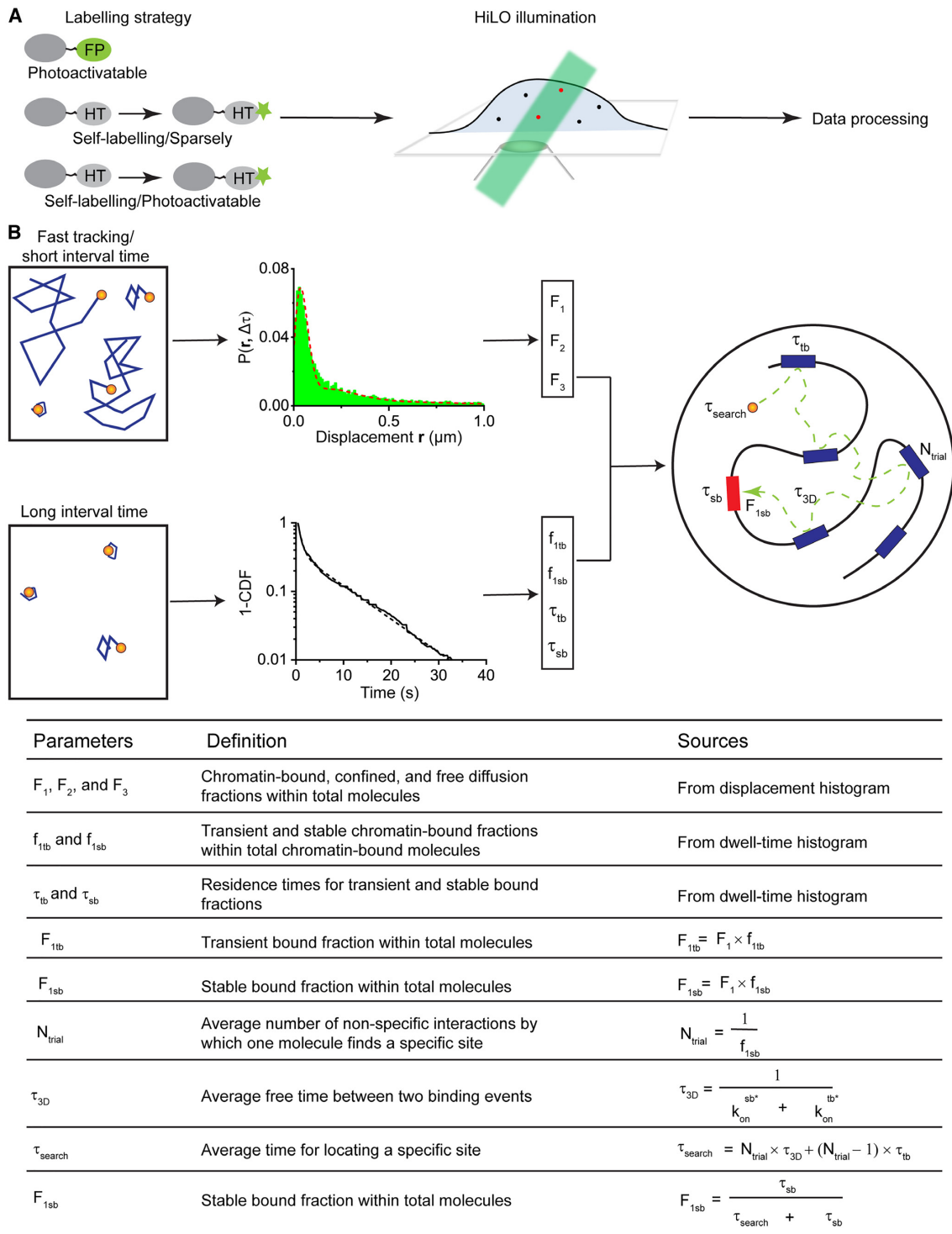
Parameters	Definition	Sources
F_1, F_2, and F_3	Chromatin-bound, confined, and free diffusion fractions within total molecules	From displacement histogram
f_{1tb} and f_{1sb}	Transient and stable chromatin-bound fractions within total chromatin-bound molecules	From dwell-time histogram
τ_{tb} and τ_{sb}	Residence times for transient and stable bound fractions	From dwell-time histogram
F_{1tb}	Transient bound fraction within total molecules	$F_{1tb} = F_1 \times f_{1tb}$
F_{1sb}	Stable bound fraction within total molecules	$F_{1sb} = F_1 \times f_{1sb}$
N_{trial}	Average number of non-specific interactions by which one molecule finds a specific site	$N_{trial} = \dfrac{1}{f_{1sb}}$
τ_{3D}	Average free time between two binding events	$\tau_{3D} = \dfrac{1}{k_{on}^{sb*} + k_{on}^{tb*}}$
τ_{search}	Average time for locating a specific site	$\tau_{search} = N_{trial} \times \tau_{3D} + (N_{trial} - 1) \times \tau_{tb}$
F_{1sb}	Stable bound fraction within total molecules	$F_{1sb} = \dfrac{\tau_{sb}}{\tau_{search} + \tau_{sb}}$

Figure 2. Schematic representation of the quantification of the target-search process. (**A**) Schematic description of live-cell SMT, including labelling, imaging, and data processing. (**B**) The 'fast-tracking'/short interval time stroboscopic SMT experiments, consisting of a short camera exposure time followed by a short camera dark time, typically with a total interval time of 5–30 ms, are performed to extract fractions and diffusion coefficients (F_1 (D_1), F_2 (D_2) and F_3 (D_3)), which represent chromatin-bound, confined, and free diffusion populations of total molecules within cells, respectively. The displacement histogram is fitted through kinetic modelling. A long interval time of 200–1000 ms and low illumination laser intensities (to minimize photobleaching) are carried out to measure residence times (τ_{tb} and τ_{sb}) as well as stable and transient bound fractions (f_{1tb} and f_{1sb}) of total chromatin-bound molecules. The dwell-time distribution is typically fitted by a two-component decay function. The stable and transient bound fractions (F_{1tb} and F_{1sb}) of total molecules within cells can be described as $F_{1tb} = F_1 \times f_{1tb}$ and $F_{1sb} = F_1 \times f_{1sb}$, respectively. N_{trial} is the average number of non-specific interactions by which one molecule undergoes before encountering a specific site ($N_{trial} = \frac{1}{f_{1sb}}$) and τ_{3D} is the average free time between two binding events ($\tau_{3D} = \frac{1}{k_{on}^{sb*} + k_{on}^{tb*}}$). The target-search time needed to find a specific site is described as $\tau_{search} = N_{trial} \times \tau_{3D} + (N_{trial} - 1)\tau_{tb}$. The relationship among the specific-bound fraction (F_{1sb}), the residence time on specific site (τ_{sb}) and the target-search time (τ_{search}) is characterized as $F_{1sb} = \frac{\tau_{sb}}{\tau_{search} + \tau_{sb}}$.

dye concentrations, visualization of individual chromatin-bound factors can be realized (45,48). Additionally, tagged proteins can be fully labelled by photoactivatable dyes. Like photoswitchable fluorescent proteins, a subset of dyes is activated to achieve single-molecule resolution (112,113).

Three common approaches have been used for expressing fusion proteins in living mammalian cells. Transient expression is the most traditional method and requires the least planning and prep work but is subject to overexpression. Stable expression involves integrating fusion genes into the cellular genome and typically uses tetracycline response elements to control the expression level of fusion proteins. Transient and stable expression places genes in a non-native location on chromatin, potentially disrupting normal gene interactions, leading to altered cellular phenotypes. Additionally, endogenous proteins may functionally compete with exogenously targeted fusion proteins. In attempts to edit genes endogenously, clustered regularly interspaced short palindromic repeats (CRISPR)-CRISPR associated protein (Cas) 9 has been altered through genetic engineering to allow for experiments in mammalian cells (114,115). CRISPR relies on short guide RNA (sgRNA) to target a specific site on chromatin for Cas9 nuclease activity. The cell uses a variety of DNA-repairing mechanisms, the most utilized being non-homologous end joining (NHEJ) of the double-stranded break, which is very efficient and results in frequent insertions or deletions (indels) within the genome, ideal for creating gene knockouts. Alternatively, homology-directed repair (HDR) allows for precise gene editing or insertion of imaging modalities (fluorophores or self-labelling tags) (114,115).

Imaging techniques

Signal-to-noise ratio (SNR) is a key factor for imaging individual molecules in the crowded, complex nucleus as low SNR limits image clarity and resolution. This is achieved by separating the pathways between excitation and emission. Highly inclined and laminated optical sheet (HILO) microscopy lowers extraneous auto-fluorescence to reduce the signal-to-noise ratio as well as enables illuminating the nucleus (116). HILO microscopy utilizes an angle of incidence shifted to the side, resulting in a highly inclined laser output. This light is laminated into a thin optical sheet through the use of a field stop at the center of the sample (specimen plane), creating a concentrated light sheet that is very thin and passes through the specimen plane, allowing for detection of individual molecules in the nucleus. The excitation and emission light pathways of HILO microscopy partially overlap, which reduces SNR, limiting its use in deep tissue single-molecule imaging.

Light-sheet fluorescence microscopy (LSFM) is an imaging set up in which the angle of incidence is horizontal through the sample instead of vertical, thus the emission and excitation light pathways are separated, which greatly increases SNR (51,117). Light-sheet microscopy allows for the imaging of samples hundreds of microns thick by illuminating the sample plane-wise (through orthogonal objectives) and appending multiple images together to form a z-stack. Because of the sheet-like illumination, this method only excites molecules that are in-focus, preserving sample integrity more efficiently than HILO and results in overall less image acquisition time. Furthermore, these microscopes can measure systems in 4D by recording 3D z-stacks over time. The limitation on resolution here is image acquisition time over the entire sample depth. To overcome this, lattice light-sheet fluorescence microscopy (L-LSFM) was developed (46,118). L-LSFM applies an optical lattice with a linear array of non-diffracting Bessel beams, which allows for greater time resolution due to parallelization of image acquisition. Spreading of foci across many points allows for reduced light intensity at any given point, leading to less overall photodamage. Multifocus microscopy enables 3D imaging in multiple colors, providing a way to track the 3D motion of single molecules at fast speed (119). Utilization of these methods has paved the way for studies that follow the dynamics of nuclear factors and has led to new insights into chromatin-associated factor activities, which is not easily available through traditional biochemical methods.

Data analysis

Live-cell SMT enables quantifying the chromatin-bound fraction, diffusion coefficient, and residence time (43,45,47–54,113,120–122) as well as target-search parameters of transcription factors and epigenetic factors in living cells by varying imaging conditions (34,44,49,52,113,120) (Figure 2B). Data analysis typically involves three steps: (i) tracking and linking, (ii) extracting the bound fraction and diffusion coefficient and measuring residence time and (3) calculating target-search parameters. To extract kinetic fractions and diffusion coefficients, 'fast-tracking' stroboscopic SMT experiments are performed. This typically consists of a short camera exposure time followed by a short camera dark time (time between consecutive frames) with a total time of 5–30 ms. The short integration time can reduce the bias of 'motion blur' because 3D freely diffusing molecules tend to 'motion blur' and can move several pixels during a short exposure time (113,123). The tracking and linking are typically performed by the MTT algorithm or the U-track algorithm (124,125), which are freely available in MATLAB-based scripts. Other custom-made tracking software is also available, such as TrackRecord (126). MTT and U-track treat individual fluorophores as point-source emitters described by the Point-Spread Function (PSF). Sub-diffraction limit resolution is achieved by fitting images with a two-dimensional Gaussian function. Particles are linked according to the distance of their consecutive positions. Kinetic fractions and diffusion constants are obtained by kinetically modelling the displacement or jump length histogram (48,51,123). Alternatively, kinetic fractions and diffusion constants can be obtained through a diffusion coefficient histogram decomposed by a multicomponent Gaussian function without kinetic modelling (45,52,127).

To measure residence/dwell times, a long interval time (camera exposure time plus dark time) of 200–1000 ms and low illumination laser intensities are used (5,46,48). A long interval time can allow the blurred images of fast diffusing molecules to blend into the background while slow-moving molecules remain clear (128,129). The slow-diffusing molecules might be chromatin-bound or confined movement populations (122). Observations indicate that

the confined populations have longer dwell times and larger diffusion coefficients than the chromatin-bound ones (122). When analyzing residence times, the confined fractions can be excluded from the bound ones based on their difference in jump distances or diffusion coefficients (45,48,122). Low illumination intensities can minimize photobleaching. Even so, photobleaching is still a major hurdle in obtaining true residence times of transcription regulatory factors (121,130). Reported residence times should be considered as apparent residence times. The dwell times of individual molecules are counted as their track length. The cumulative frequency distributions of dwell times are normalized for photobleaching (48,121). The normalized cumulative frequency distributions are fitted with single-, two- or three-component exponential decay (34,43–54,113,120,131) or power-law (52,121,122) functions. The exponential decay model hypothesizes that transcription regulatory factors bind different sites with distinct affinities. For instance, a two-component exponential model assumes that transcription regulatory factors have three states: freely diffusing, short-lived, and long-lived. The short- and long-lived populations are often assigned as non-specifically and specifically bound ones, respectively; however, the assumption should be tested using exquisite controls from *in vitro* and *in vivo* experiments. The power-law model hypothesizes that transcription regulatory factors bind chromatin with a broad distribution of binding affinities (121,122). This model fits 1D cumulative distributions of dwell times better than the exponential model (121,122), but fails to generate time-related kinetic parameters that describe processes of biochemical reactions. The broad distribution of binding affinities presents a challenge for unbiased sampling of all binding events. Thus, it is critical to perform control experiments using Tags (control for transient binding) and histone proteins (control for stable binding). In addition, generating variants that can eliminate specific populations is an exquisite control for estimating residence time. By kinetic modelling of transcription regulatory factors occupying the three different states assumed, target-search parameters, including the number of non-specific sites sampled, the 3D freely diffusing time between two binding sites, and the time for locating stable bound sites can be estimated (34,44,49) (Figure 2B).

BINDING MECHANISMS: EPIGENETIC MODIFICATIONS VERSUS GENETIC ELEMENTS

Binding of the CBX-PRC1 complexes to chromatin

The CBX-PRC1 complexes contain multiple subunits that could cooperatively contribute to the targeting of them to cognate sites by multivalent engagement of chromatin (132–134). Nevertheless, observations from live-cell SMT indicate that the CBX proteins bind more stably to chromatin than RING1B, MEL18 and PHC1 (34,45,135). This suggests that the CBX proteins directly associate with chromatin and that other CBX-PRC1 subunits bind chromatin through the CBX proteins. Consistently, depletion of other CBX-PRC1 subunits have minor or no effects on the binding of CBX to chromatin (34,45). Mutation of the chromatin-binding module of RING1B does not impact its binding stability (135). These results point out that binding

of CBX-PRC1 complexes to chromatin is mediated by the CBX proteins.

The prevailing model concerning how CBX proteins are targeted to chromatin is that the chromodomain of CBX proteins binds H3K27me3. Structural studies have shown that the CBX chromodomain binds H3K27me3-peptides (91). Paradoxically, biophysical studies have indicated that the CBX chromodomains have a very weak or undetectable affinity for H3K27me3 and cannot distinguish H3K9me3 from H3K27me3 (91–93). Genome-wide studies have demonstrated that CBX-PRC1 proteins sharply locate within broad H3K27me3 domains (136). These data indicate that multiple mechanisms are involved in targeting CBX-PRC1 to cognate sites, consistent with the structural and functional diversity of the CBX proteins (12), which is further supported by live-cell single-molecule imaging of the CBX proteins. Live-cell SMT observations demonstrate that H3K27me3 controls the targeting of CBX7 and CBX8 to chromatin but has minor effects on CBX2, CBX4 and CBX6 (34,45) (Figure 3A).

How does a weak affinity of CBX7 for H3K27me3 direct its stable association with and selective location within sub-regions of broad H3K27me3 domains? Single-molecule observations show that the removal of H3K27me3 almost completely diminishes the binding of CBX7 to chromatin and that the deletion of CD, the domain recognizing H3K27me3, greatly reduces the level of CBX7 on chromatin (45). These results suggest that H3K27me3 plays a critical role in controlling the chromatin-bound level of CBX7-PRC1. Consistently, Huseyin et al. indicated that the depletion of SUZ12 of PRC2 results in a reduction in the total chromatin-bound fraction of MEL18 and RING1B, both of which are the core components of CBX7-PRC1 (135). Biophysical studies have shown that CBX7 binds DNA through its AT-hook motif (45). Live-cell SMT reveals that the AT-hook motif is important for stabilizing CBX7 on chromatin (45). It may be speculated that the targeting of CBX7 to chromatin is dependent on co-recognition of DNA and H3K27me3. H3K27me3 may act as an allosteric effector that promotes binding of CBX7 to chromatin through DNA interactions. Implicit in this model is that the binding of CBX7 to DNA is auto-inhibited by unknown mechanisms and is allosterically regulated by their interaction with H3K27me3. H3K27me3 also allosterically stimulates PRC2 methyltransferase activity (64,137). Collectively, these observations suggest that H3K27me3 is an allosteric effector that directs CBX7-PRC1 binding as well as PRC2 enzymatic activity.

CBX2 is the driver and nucleator of liquid–liquid phase separation of the CBX-PRC1 complexes (32–34), suggesting that CBX2 may nucleate at the specific chromatin regions that provide sites for stabilizing CBX2 on chromatin. The binding of CBX2 to chromatin can slow down its diffusion and increase its local concentration, thereby driving phase separation. H3K27me3 and CBX2-PRC1 subunits contribute little to the binding stability of CBX2 (34). Observations from live-cell SMT indicate that CBX2 nucleates on chromatin through the AT-hook motif, which interacts with underlying DNA elements of chromatin (34). CBX2 interaction with DNA is essential for liquid–liquid phase separation (LLPS) of CBX2
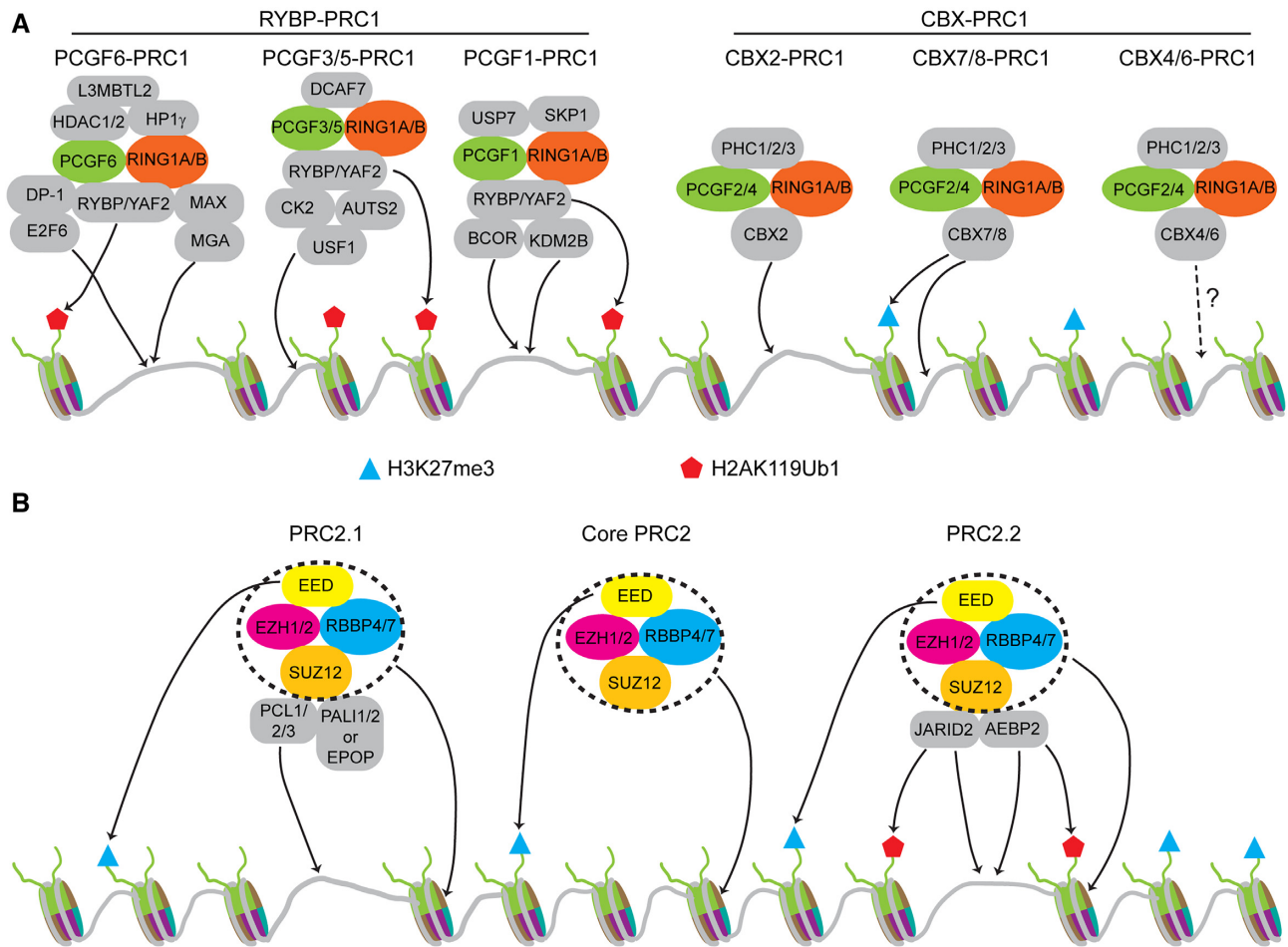
Figure 3. Binding mechanisms of PRC1 and PRC2. (**A**) Binding of PRC1 to chromatin. The RYBP and YAF2 subunits of RYBP-PRC1 recognize H2AK119Ub1, which promotes RYBP-PRC1 ubiquitin ligase activity. PCGF1-PRC1, PCGF3/5-PRC1, and PCGF6-PRC1 are stabilized at chromatin through interaction with DNA (BCOR and KDM2B for PCGF1-PRC1, USF1 for PCGF3/5-PRC1, and DP-1, E2F6, MAX and MGA for PCGF6-PRC1). CBX2-PRC1 binds to chromatin mainly through CBX2 interaction with DNA and H3K27me3 makes a minor contribution to the binding (not shown). CBX7- and CBX8-PRC1 co-recognize H3K27me3 and DNA. The molecular mechanisms underlying CBX4- and CBX6-PRC1 binding remain to be characterized. The arrowhead curves indicate that complexes recognize specific features of chromatin. The dashed arrowhead curves indicate that the molecular mechanisms underlying complex stabilization remain unclear. (**B**) Binding of PRC2 to chromatin. The core PRC2 complex (dashed circle) has intrinsic chromatin-binding activity, mainly through interaction with DNA. The EED subunit of PRC2 recognizes H3K27me3, which promotes PRC2 methyltransferase activity. PRC2.1 is stabilized at chromatin by PCL interaction with CpG-rich DNA. JARID2 and AEBP2 recognize both CpG-rich DNA and H2AK119Ub1, which stabilizes PRC2.2 at chromatin and promotes its activity.

(34). Further studies are needed to identify the DNA sequences within the genome needed for CBX2 nucleation. CBX2 also binds RNAs through the same region that binds DNAs (138). Observations from *Drosophila* show that RNAi components are required for nuclear clustering of Polycomb group response elements (39). Recent results indicate that RNAs are involved in the regulation of transcriptional condensates (139). It would be interesting to test whether the biogenesis of Polycomb condensates requires RNA.

Another interesting observation is that over 90% of CBX2 stably binds to mitotic chromosomes without dissociation (140). This binding directly recruits the canonical PRC1 components to mitotic chromosomes (140). The mitotic immobilization of CBX2 may be involved in chromosomal segregation and instability (141). Additionally, CBX2 can directly bind to and compact reconstituted nu-

cleosomes (95). Thus, these observations suggest CBX2 directly binds chromatin through interaction with DNA. The removal of H3K27me3 does not influence the binding stability of CBX2 on chromatin; however, H3K27me3 impacts the search efficiency of CBX2 (34). These data suggest that CBX2 may recognize H3K27me3, though the recognition may not be the main driver of its interaction with chromatin. Since the genomic occupancy of chromatin-associated factors is determined by binding stability and target-search efficiency (44,49,113), it is possible that CBX2 integrates genetic and epigenetic information to regulate its genomic occupancy.

Overall, available results support a model by which the CBX-PRC1 proteins integrate genetic and epigenetic information to locate their target sites. Given that epigenetic complexes recognize epigenetic modifications and genetic DNA sequences, this information integration could be a

generic mechanism underlying targeting of epigenetic complexes to chromatin.

Binding of the RYBP-PRC1 complexes to chromatin

Unlike the CBX-PRC1 complexes, the RYBP-PRC1 complexes contain accessory subunits that have characteristic DNA or chromatin binding activities, which target them to Polycomb domains (87,89,100,103–107) (Figure 3A). Recently, Huseyin et al. endogenously Halo-tagged PCGF1/3/6 and studied their dynamics by SMT in living cells (135). Given the composition of PCGF3-PRC1 being similar to PCGF5-PRC1 (87,89), PCGF5 was not included in the study. Observations indicate that PCGF1 has the highest chromatin-bound fraction and that PCGF3 and PCGF5 have smaller bound fractions than RING1B (135). They also showed that PCGF1 does not stably associate with chromatin (135) when its terminal RAWUL domain, which interacts with chromatin binding subunits BCOR and KDM2B (103–105,142), is removed. It would be interesting to investigate whether and how BCOR and KDM2B individually or cooperatively contribute to the binding stability and specificity of PCGF1-PRC1 on chromatin, thereby affecting PCGF1-PRC1 ubiquitin ligase activity. PCGF6-PRC1 has four accessory transcription factors (DP-1/E2F6/MAX/MGA) that recognize specific DNA elements, along with HP1γ which recognizes H3K9me3 (100,106,107). These transcription factors regulate the specificity of PCGF6-PRC1; however, it is unclear whether and how these transcription factors and HP1γ cooperatively regulate their binding stability. The PCGF3/5 proteins are not significantly enriched at Polycomb target genes (100) and are primarily responsible for deposition of a low level of H2AK119Ub1 across the genome (101). PCGF3 binds to chromatin with a residence time of ∼40 s (135), suggesting that the association of PCGF3/5-PRC1 complexes with chromatin may facilitate a low-level deposition of H2AK119Ub1 throughout the genome. PCGF1/6 bind more stably to chromatin than PCGF3 (135). The residence time of PCGF3 measured in (135) is much longer than other PRC1 subunits reported in (34,44,45). The discrepancy could be due to experimental approaches and data analysis aforementioned. Nevertheless, the distinct targeting and binding mechanisms among the RYBP-PRC1 complexes may be important for catalysis and the appropriate distribution of H2AK119Ub1 in the genome.

Binding of the PRC2 complexes to chromatin

The core of PRC2 associates with auxiliary proteins to form PRC2.1 and PRC2.2 (89). SUZ12 is the scaffold protein that mutually exclusively associates with accessory proteins to define PRC2.1 (core + PCL1–3 + EPOP or PAL1) and PRC2.2 (core + AEBP2 + JARD2) (68,85,86,137,143) (Figure 3B). By introducing SUZ12 mutants that disrupt the interactions with PHF1 (PCL3), AEBP2, or both into SUZ12-knockdown cells, observations from live-cell SMT indicate that the chromatin-bound fraction of EZH2 is greatly reduced (67). In agreement with this, the deletion of the EZH2 SANT2 domain, which interacts with SUZ12, greatly reduces both the residence time and chromatin-

bound fraction (44). These data suggest that the PRC2 auxiliary proteins stabilize PRC2 on chromatin, consistent with the genome-wide ChIP-seq studies (68,85,86).

How do the PRC2 auxiliary proteins stabilize the core PRC2 on chromatin? An *in vitro* single-molecule colocalization study provides insights into the underlying mechanism (144). Studies show that PRC2 preferentially binds free DNA with a few second residence time and nanomolar affinity (144). Consistently, biochemical studies demonstrate that PRC2 binds naked DNA better than nucleosomes (145). PHF1, an accessory protein of PRC2.1, is a DNA binding protein (77,78). Interestingly, PHF1 can prolong the PRC2 residence time by 3-fold (144). The disruption of the DNA-binding capacity of PHF1 results in a reduction in the residence time of PRC2 as well as the methyltransferase activity (144), suggesting there is a correlation between the residence time and the PRC2 enzymatic activity.

PRC2 recognizes epigenetic marks such as H3K27me3, H2AK119Ub1 and H3K36me3 (137,146,147) (Figure 3B). Do these epigenetic marks contribute to PRC2 stabilization on chromatin? To test the role of H3K27me3 in PRC2 binding, Youmans *et al.* established cell lines with endogenously Halo-tagged EZH2 (67). When treating cells with a small molecule (A-395), which inhibits the interactions between EED and H3K27me3 without affecting the H3K27me3 level, by using live-cell SMT, they found that the residence time of EZH2 is similar to that in control cells (67). In agreement with this, studies from the same group demonstrate that H3K27me3 has no apparent effects on PRC2 binding when using reconstituted nucleosomes as substrates (145). These results suggest that the recognition of epigenetic markers by PRC2 may function as allosteric effectors rather than binding stabilizers.

In summary, similar to PRC1, PRC2 integrates genetic and epigenetic information to determine its binding stability and enzymatic activity, which is consistent with the concept by which epigenetics link genetics to the environment and disease (148).

Methylation of the genome by the PRC2 complexes

PRC2 is the methyltransferase that is responsible for methylation of more than 80% of all histone H3 across the genome (61,66). 5–10% of all histone H3 is found to be H3K27me1 occurring within gene bodies of actively transcribed genes. 50–70% of histone H3 is H3K27me2 enriched at inter- and intra-genetic regions, which prevents inappropriate promoter or enhancer activity. 5–10% of all histone H3 is trimethylated to produce H3K27me3, which is strongly enriched at PRC2 binding sites (61,66,149,150). Other genomic regions also contain dispersed/diffusive H3K27me3 with an average 4- to 5-fold lower than target regions (66,85). Interestingly, by using ChIP-seq, PRC2 proteins are detectable at target regions rather than H3K27me1-, H3K27me2- and dispersed H3K27me3-regions (61,66,149).

It remains incompletely understood how PRC2 deploys a degree of H3K27 methylation at different regions across the genome. Recent observations from live-cell single-molecule imaging may provide some insights into the methylation process of PRC2. Two independent observations indicate

that ∼20% of PRC2 core components associate with chromatin (44,67). Notably, ∼5% of PRC2 stably binds to chromatin while 16% of PRC2 transiently binds to chromatin (44). It is likely that the stable bound fraction of PRC2 is primarily responsible for trimethylation of Polycomb target regions and the transient bound population may be responsible for mono- and di-methylation of histone H3. It would be interesting to address this assumption in the future.

What are the molecular features of stable and transient bound fractions of PRC2 within cells? The core PRC2 complex associates with sub-stoichiometric components to produce PRC2.1 and PRC2.2 (61). These auxiliary proteins promote the core of PRC2 activity and association with chromatin (Figure 3B). Interestingly, removal of all accessory proteins prevents preferential trimethylation of histone H3 at target regions but does not affect the global level of H3K27me3 as well as H3K27me1 and H3K27me2 (85,86). Consistent with this, the C-terminal VEFS domain of SUZ12 is sufficient to form a catalytic complex with EED and EZH2, which achieves the global level of H3 methylation except for H3K27me3 at target regions but cannot be detected by ChIP-seq (66). These observations suggest that there may be three complexes coexisting within cells, core PRC2, PRC2.1 and PRC2.2 (Figure 3B). The core PRC2 activity is responsible for the global level of H3 methylation while PRC2.1 and PRC2.2 trimethylate H3 at target regions. We propose that the core PRC2 is the transient bound fraction and PRC2.1 and PRC2.2 are stable ones, consistent with that the recombinant core PRC2 binds to chromatin more dynamically than the recombinant PRC2.1 (144). This hypothesis is also consistent with the observation that a prolonged residence time by PHF1 promotes the PRC2 methyltransferase activity (144).

A HIGHLY DYNAMIC PRC1 SYSTEM WITH LOW TARGET-SITE OCCUPANCY

Genome-wide ChIP-seq provides a static distribution of Polycomb proteins along chromatin with a limited stoichiometric relationship. Nevertheless, the absolute occupancy level is fundamentally important for understanding the mechanisms that underpin how the Polycomb system establishes repressive Polycomb domains. Tatavosian et al. developed a method termed single-molecule chromatin immunoprecipitation imaging (Sm-ChIPi) that enables counting the number of proteins on chromatin (151). Sm-ChIPi combines chromatin immunoprecipitation with the power of single-molecule imaging to count the number of fluorescently labelled proteins through analysis of photobleaching steps or florescence intensity (151). By using Sm-ChIPi, it was found that one PRC1 complex associates with multiple nucleosomes (151), suggesting a low target-site occupancy level of PRC1 on chromatin. Recently, Huseyin *et al.* estimated the number of PRC1 proteins on chromatin based on the number of endogenously Halo-tagged PRC1 molecules in cells quantified by immunoblotting and their chromatin-bound fraction obtained from live-cell SMT (135). They found that one RNIG1B molecule occupies, on average, every 10 kb of RING1B-enrcihed chromatin (135). Despite the discrepancy of the absolute stoichiometry between the two studies, which could be due to experimental ap-

proaches, these data suggest that PRC1 sparsely binds target sites in the genome and dynamically engages with chromatin. This dynamic engagement could be advantageous in modifying chromatin and regulating chromatin structure since it requires a small number of proteins in the system. Given that many epigenetic complexes are highly dynamic, it would be interesting to test whether other epigenetic complexes employ similar sparse binding mechanisms to engage chromatin.

TARGET-SEARCH: SAMPLING MECHANISMS AND ITS REGULATION BY PHASE SEPARATION

The origin of target search: transcription factors

Transcription regulatory factors must efficiently locate their cognate sites (3–6). One of the fundamental questions in the transcription field is how transcription regulatory factors locate their cognate sites within the genome. It is challenging to locate specific sites because a myriad of non-specific sites occur within the genome. Early studies reveal that transcription factors rapidly locate their cognate sites (152), which is achieved by alternating between 3D diffusion in solution and 1D diffusion along DNA, a process termed 'facilitated diffusion' (153). The 1D diffusion involves three possibilities: (i) 1D sliding by which transcription factors slide along DNA by continually associating with DNA; (ii) 'jumping' (steps >100 bp) or 'hopping'(steps <10 bp) by which transcription factors transiently dissociate from DNA; and (iii) intersegmental transfer by which a transcription factor bound to a DNA site transfers to another site *via* an intermediate state in which it is transiently bound to both (3,4). The facilitated diffusion model suggests that the 1D diffusion along DNA dominates the target-search process. Consistently, Elf et al. demonstrated that the *lac* repressor spends ∼90% of time nonspecifically bound to and diffusing along DNA in a living *Escherichia coli* cell (129). The lac repressor slides ∼45 bp on DNA and the sliding can be obstructed by roadblocks − other DNA binding proteins (154).

The sizes of mammalian genomes are much larger than *Escherichia coli*. What are the mechanisms underlying how mammalian transcription factors explore and locate their cognate sites? In mammals, nucleosomes are roadblocks for transcription factors sliding along DNA and impact facilitated diffusion. Similar to the *lac* repressor in prokaryotic cells, live-cell SMT observations indicate that the transcription factor p53 locates its cognate sites through alternating between 3D free diffusion in the nucleoplasm and 1D diffusion along DNA in mammalian cells (49). However, unlike the *lac* repressor in prokaryotic cells, p53 uses a 3D diffusion–dominant target search mechanism. The p53 protein takes ∼100 s to locate its target sites and spends more than 80% of time in 3D free diffusion (49). Transcription factors often cluster through intra- and/or inter-molecular interactions of intrinsically disordered regions encoded in activation domains (155). These compartments could facilitate the target-search process through increased local protein concentrations and enriched target sites within clusters. Live-cell SMT shows that Sox2 hops between binding sites within clustered regions (130). Single-molecule imaging also indicates that compartmentalizing of RNA poly-

merase II or clustering of CTCF facilitates the efficiency of the target-search process (120,156). CTCF is repeatedly trapped in CTCF clusters in which CTCF is more likely to move backward in the opposite direction than to continue forward (120). The trapping increases the efficiency of CTCF target search by ~2.5-fold, suggesting that local clusters of DNA-binding proteins can speed up their target-search rate (on-rate) to locate cognate binding sites (120). Thus, an emerging model is that transcription factors employ a 3D-dominant target-search mechanism to explore mammalian genomes and the exploration is accelerated by spatial organization of cognate sites and transcription factors (120). Since transcription factors and coactivators can form condensates *via* LLPS (157–160), it would be interesting to dissect functional relationships between LLPS-mediated condensate formation, target localization, and transcription activity.

PRC1 and PRC2 sample the genome to locate target sites

Unlike transcription factors that interact with DNA in a sequence-specific manner, epigenetic factors associate with chromatin through multivalent engagement of histone and DNA modifications, non-coding RNAs and DNA sequences (132–134). Epigenetic factors should integrate epigenetic and genetic information to locate their target sites. Upon utilization of live-cell SMT, it was found, similar to transcription factors, that the PcG complexes employ a sampling mechanism to locate their target sites by exploring the nucleus through alternation between 3D free diffusion and sampling the genome (34,44) (Figure 2B). The term 'sample' reflects that epigenetic factors locating cognate sites is instructed by chromatin environments determined by transcription activity, epigenetic information, genetic DNA, and others. These single-molecule data are consistent with a sampling mechanism proposed previously (161,162). By assuming two binding states (transient versus stable) and performing kinetic modelling, it is possible to estimate target-search time (time spent by proteins alternating between transient binding and 3D free diffusion to reach a stable site) (34,44,49) (Figure 2B). 3D free diffusion time is the average free time between two binding events, which is the inverse of on-rate. The number of transient sites sampled is the average number of trials by which one molecule needs to encounter a stable site. It should be noted that live-cell SMT might not be able to detect very brief contacts of PcG proteins with chromatin. The sampling number should be considered as a minimum. Although CBX-PRC1 and PRC2 exploit similar sampling mechanisms to explore chromatin states, CBX-PRC1 is more efficient in locating target sites than PRC2. After dissociating from a transient site, PRC1 takes ~70 s to locate the next stable site while PRC2 spends ~200 s finding another specific site, which is because CBX-PRC1 spends a shorter time in 3D free diffusion than PRC2. The PcG complexes sample ~5.0 non-specific sites to reach a specific site and reside ~4.0 s on non-specific sites, indicating that the 3D free diffusion time is much longer than the 1D sliding time. This suggests that 3D free diffusion dominates the target-search process, which is similar to transcription factors in mammalian cells but different from prokaryotic cells. The different target-search efficiency be-
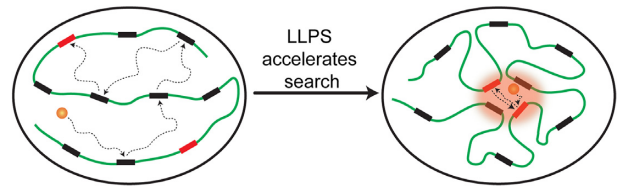

Figure 4. LLPS accelerates the target-search kinetics of CBX2. Phase separated Polycomb condensates speed up CBX2 locating its stable sites by reducing the 3D free diffusion time (the major time factor in target-search) and the number of non-specific trials between specific binding events, thereby enhancing its genomic occupancy.

tween PRC1 and PRC2 may reflect that PRC2 is the enzyme for sampling chromatin states to deposit H3K27me3, which facilitates CBX-PRC1 sampling.

Phase-separated condensates accelerate target search

There are multitudes of biochemical reactions occurring simultaneously in the nucleus to control the metabolism of nucleic acids. Mammalian cells utilize numerous membraneless condensates to compartmentalize these biochemical reactions in order to achieve the efficiency and specificity of nucleic acid metabolism (10,163). Many membraneless condensates are assembled via LLPS (164–166). It has been suggested that phase-separated condensates accelerate biochemical reactions (164–166). Results from *in vitro* experiments support this major function of condensates (167); however, there is a lack of direct *in vivo* evidence, partly due to the unavailability of techniques that measure reaction kinetics in live cells.

Recent observations indicate that phase-separated condensates accelerate the target-search efficiency of epigenetic factors (34). CBX2 may be the driver of PRC1 to phase separate to form condensates (32–34). This provides a way to manipulate the formation of condensates through mutating CBX2. By utilizing live-cell SMT and genetic manipulation, Kent *et al.* demonstrated that CBX2 employs a sampling mechanism to locate its target sites by exploring the nucleus through alteration between 3D free diffusion and sampling the genome (34) (Figure 4). The 3D free diffusion time of CBX2 is much longer than the 1D sliding time, suggesting that 3D free diffusion dominates the target-search process and reducing 3D diffusion may be a way to achieve a high genomic occupancy. Notably, the molecular process by which CBX2 samples target sites inside condensates is distinct from that outside condensates. CBX2 is more likely to move backward inside condensates than outside condensates. This facilitates CBX2 to revisit the same or adjacent sites repeatedly inside condensates. Repetitive visiting of the same or adjacent binding sites reduces the length of 3D free diffusion time and the sampling of transient sites, which is consistent with CTCF exploring its cluster (120). At the molecular basis, the repetitive visits could be due to intersegmental transfer since CBX2 can self-organize. Another possibility is that condensates facilitate CBX2 hopping and jumping. It would be interesting to address these potential mechanisms in the future.

When responding to developmental signals and stress stimuli, cells adapt to these intra- and extra-cellular sig-

nals through transcription regulation. Transcription regulation is typically achieved by controlling occupancy level of transcription factors and/or epigenetic regulators on chromatin. Interestingly, the genomic occupancy level of chromatin-binding factors can be regulated by phase-separated transcription condensates (34). Condensates can enhance the genomic occupancy level of CBX2 by ∼4.0-fold through speeding up its target-search process without influencing residence time. Since LLPS can rapidly respond to environmental stimuli and stresses, such as pH and temperature (164–166), and provide specificity through compartmentalization (164–166), LLPS could be a generic mechanism to achieve efficiency and specificity of nucleic acid metabolism.

A PHASE-SEPARATION MODEL FOR GENOME OR-GANIZATION BY CBX-PRC1

Nucleation of CBX2-PRC1 condensates by DNA elements

Phase-separated condensates are implicated in genome organization to activate or repress transcription. For gene activation, transcription factors, coactivators, and RNA polymerase II coordinately assemble transcription condensates to activate transcription (139,157–160,168–174). For gene repression, heterochromatin protein (HP) 1 phase separates to assemble condensates that organize constitutive heterochromatin (175–178). However, observations also indicate that the formation of heterochromatin foci is independent of HP1 (179). Further studies are needed to resolve these discrepancies. CBX2 phase separates *in vitro* and *in vivo*, suggesting that LLPS may be involved in the formation of facultative heterochromatin (32–34). Additionally, chromatin phase separates to form liquid-like condensates, which can be regulated by epigenetic modifications (180). Despite these exciting advances, the molecular mechanisms underlying how LLPS organizes the genome for transcription regulation remain enigmatic. To activate or repress gene expression, transcriptional condensates should localize at specific sites of the genome and be able to pull together distal regions (181–184). Spatial localization of transcription condensates could occur through a nucleating mechanism by which nuclear factors bind to specific regions of the genome (170,185). This increases residence time and reduces diffusion, thereby facilitating interactions between nuclear factors to assemble transcription condensates. Consistently, recent studies suggest that the binding of transcription factors to super-enhancers drives the localized formation of transcriptionally active condensates (170).

Although the classical view is that CBX-PRC1 is recruited to chromatin via H3K27me3 (12), the elimination of H3K27me3 does not impact the residence time of CBX2 on chromatin or prevent the formation of CBX2 condensates (34). In agreement with this, the depletion of SUZ12, the core subunit of PRC2, has a very modest effect on the condensate formation of RING1B and PCGF2 (135). The knockout of RING1A/RING1B or BMI1/MEL18 does not affect the residence time of CBX2, indicating that the CBX2-PRC1 core subunits may play less important roles in stabilizing CBX2 on chromatin. Observations further indicate that CBX2 can form condensates independently of RING1A/RING1B or BMI1/MEL18 (32–34). If the core

subunits of CBX2-PRC1 and H3K27me3 play a lesser role in binding stability, CBX2 likely is a binder for CBX2-PRC1 on chromatin, which is critical for nucleation of condensates on chromatin. Observations indicate that CBX2 is stabilized on chromatin through the AT-hook motif interacting with the underlying DNA elements of chromatin (34). Deleting or mutating the AT-hook motif completely prevents the LLPS of CBX2 in live cells (34). These studies suggest that the genetic DNA sequences may be the main driver for nucleating CBX2-PRC1 on chromatin for LLPS. In the absence of PRC2 and PRC1 core subunits, CBX2 can undergo LLPS to form condensates in cells; however, their size and locations are altered (34,135) to some extent, suggesting that PRC2 and the complex formation of CBX2-PRC1 can regulate the biogenesis of Polycomb condensates.

A scaffold-adapter-client phase separation model for organizing Polycomb target genes

The canonical CBX-PRC1 complexes compact chromatin and mediate higher-order chromatin structures (26,27,29–31,95,96,186). Recent observations in mouse embryonic stem (mES) cells provide insights into this organization. There are five CBX proteins in mES cells; however, CBX4 and CBX8 are not expressed (97) and CBX6 does not form condensates (34,187). Both CBX2 and CBX7 form condensates in mES cells (34,135,187). CBX2 is the driver of LLPS of CBX-PRC1 and CBX7 forms condensates without undergoing LLPS in live cells (33,34). CBX7 is recruited to chromatin by H3K27me3 (45) while CBX2 binds to chromatin through interaction with DNA (34). CBX2 compacts chromatin through positively charged residues (95,96), which are also critical for LLPS (32,33). The PHC subunits can polymerize *via* head-to-tail interaction of the SAM domain (94). The SAM domain of *Drosophila* Ph can also undergo LLPS (35). All together, these observations suggest a scaffold-adapter-client model by which the CBX-PRC1 complexes integrate genetic information and epigenetic modifications to organize the genome through LLPS (Figure 5).

It is plausible to assign CBX2-PRC1 as the scaffold, CBX7-PRC1 as the adapter, and H3K27me3-marked chromatin as the client. CBX7-PRC1 (adapter) recruits H3K27me3-marked region (client) into CBX2-PRC1 (scaffold) condensates through the interactions between CBX7 and H3K27me3 and PHC polymerization between CBX2-PRC1 and CBX7-PRC1. Consistent with this, the polymerization of PHC is critical for the long-range interactions of Polycomb genes as well as condensate formation (27,30,38). It is also possible that H3K27me3-marked chromatin is brought into CBX2-PRC1 condensates through the LLPS of PHC proteins (35). Although we propose that CBX2 is the scaffold and driver of Polycomb condensates, it should be noted that components of client and adapter might contribute to the biogenesis of Polycomb condensates through weak phase separation capacities or direct interactions.

This model explains how CBX7-PRC1 and H3K27me3 can be enriched in CBX2-PRC1 condensates with no or weak capacities to LLPS. The model presented here can also explain how PRC2 and RYBP-PRC1 influence long-range interactions (26–30). Both PRC2 and RYBP-PRC1 can af-
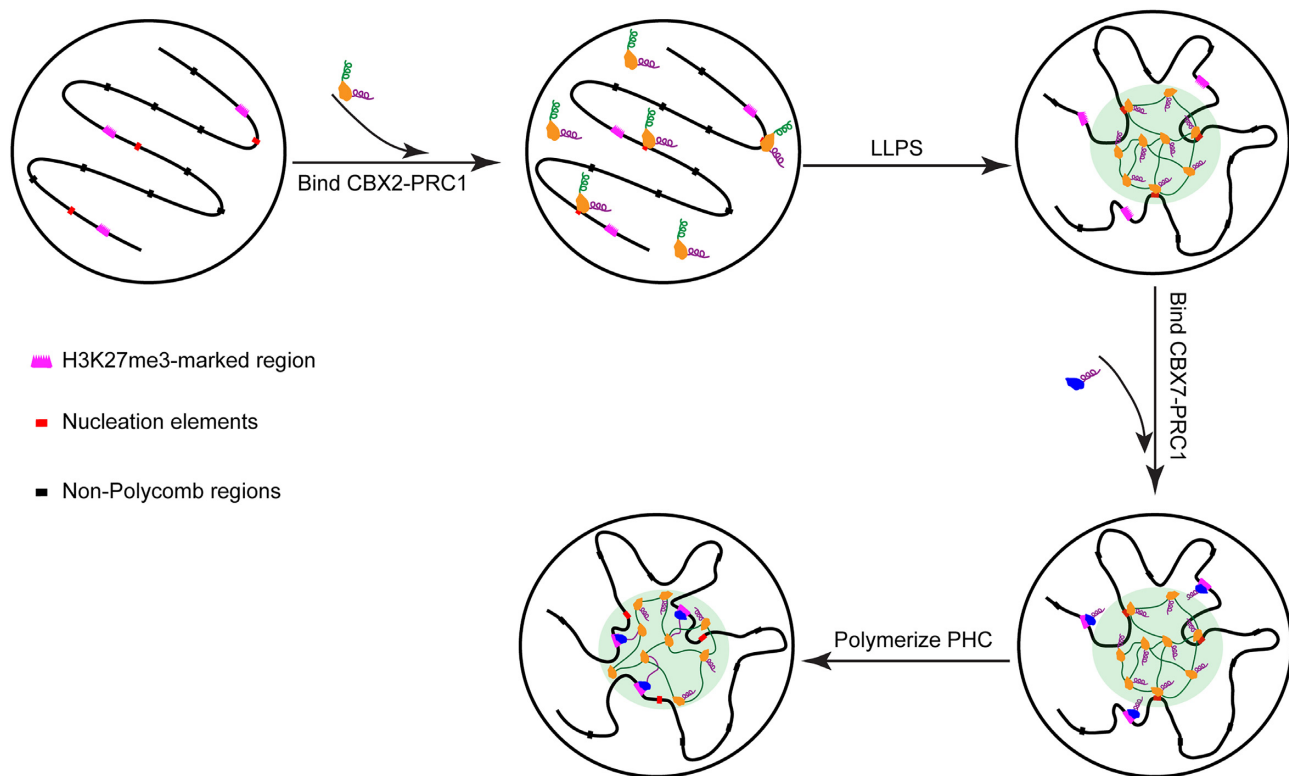
Figure 5. A scaffold-adapter-client phase separation model for organizing Polycomb genes in mES cells. Within the model, CBX2-PRC1 is the scaffold, CBX7-PRC1 is the adapter, and H3K27me3-marked chromatin is the client. CBX2-PRC1 phase separates to form condensates, which is driven by CBX2. CBX7-PRC1 recruits H3K27me3-marked regions into CBX2-PRC1 condensates through the interactions between CBX7 and H3K27me3 and PHC polymerization between CBX2-PRC1 and CBX7-PRC1, thereby bringing the client (H3K27me3-marked chromatin) into the scaffold (CBX2-PRC1 condensates). This model is based on observations from mES cells in which CBX4 and CBX8 are not expressed. CBX6 occupies a small fraction of Polycomb targets. At this stage, we cannot exclude the possibility of some clients having weak phase separation capacities. Thus, both direct interactions and composition-dependent phase separation among Polycomb subunits (PRC1 and PRC2) and Polycomb targets could contribute to the biogenesis of Polycomb condensates. The current model implies a sequential binding event, but it is possible that the order of binding events is different from the proposed model.

fect the deposition of H3K27me3 (61), thereby affecting the CBX7-PRC1 adapter interaction with H3K27me3. Thus, distal regions cannot be brought into the CBX2-PRC1 condensates through CBX7 interaction with H3K27me3 and PHC polymerization or phase separation. The scaffold-adapter-client phase separation model integrates genetic DNA and epigenetic information and unifies previous genomic and genetic observations.

CONCLUDING REMARKS

Recent biochemical and structural studies have provided insights into the catalytic activity of the PcG complexes and their regulation (137,143,188,189). Combinations of genetic engineering and ChIP-seq have uncovered the genomic locations of the PcG complexes and uncovered many factors that modulate their locations (66,85,86,100,101,108). The emerging model is that PRC1 and PRC2 form a self-enforcing feedback loop to enhance their respective activities to establish and maintain Polycomb domains. Recent live-cell SMT indicates that the PcG proteins are highly dynamic within cells and have distinct dynamic populations that interact with chromatin with different residence times. The distinct dynamic populations may be responsible for

modifying different regions of the genome. Phase-separated condensates can facilitate the efficiency of target search of Polycomb proteins. An efficient search may be essential for achieving a sufficient level of PcG proteins at Polycomb target sites as well as controlling the spreading of H3K27me3 and H2AK119Ub1, highlighting the significance of nuclear organization in regulating efficiency and specificity of nucleic acid metabolism.

REFERENCES

1. Li,B., Carey,M. and Workman,J.L. (2007) The role of chromatin during transcription. *Cell*, **128**, 707–719.
2. Kouzarides,T. (2007) Chromatin modifications and their function. *Cell*, **128**, 693–705.
3. Halford,S.E. (2009) An end to 40 years of mistakes in DNA-protein association kinetics? *Biochem. Soc. Trans.*, **37**, 343–348.
4. Normanno,D., Dahan,M. and Darzacq,X. (2012) Intra-nuclear mobility and target search mechanisms of transcription factors: a single-molecule perspective on gene expression. *Biochim. Biophys. Acta*, **1819**, 482–493.
5. Suter,D.M. (2020) Transcription factors and DNA play hide and seek. *Trends Cell Biol.*, **30**, 491–500.
6. Lionnet,T. and Wu,C. (2021) Single-molecule tracking of transcription protein dynamics in living cells: seeing is believing, but what are we seeing? *Curr. Opin. Genet. Dev.*, **67**, 94–102.
7. Yu,M. and Ren,B. (2017) The three-dimensional organization of mammalian genomes. *Annu. Rev. Cell Dev. Biol.*, **33**, 265–289.
8. Hansen,A.S., Cattoglio,C., Darzacq,X. and Tjian,R. (2018) Recent evidence that TADs and chromatin loops are dynamic structures. *Nucleus*, **9**, 20–32.
9. Misteli,T. (2020) The self-organizing genome: principles of genome architecture and function. *Cell*, **183**, 28–45.
10. Meldi,L. and Brickner,J.H. (2011) Compartmentalization of the nucleus. *Trends Cell Biol.*, **21**, 701–708.
11. Simon,J.A. and Kingston,R.E. (2013) Occupying chromatin: Polycomb mechanisms for getting to genomic targets, stopping transcriptional traffic, and staying put. *Mol. Cell*, **49**, 808–824.
12. Blackledge,N.P., Rose,N.R. and Klose,R.J. (2015) Targeting Polycomb systems to regulate gene expression: modifications to a complex story. *Nat. Rev. Mol. Cell Biol.*, **16**, 643–649.
13. Schuettengruber,B., Bourbon,H.M., Di Croce,L. and Cavalli,G. (2017) Genome regulation by Polycomb and Trithorax: 70 years and counting. *Cell*, **171**, 34–57.
14. Piunti,A. and Shilatifard,A. (2021) The roles of Polycomb repressive complexes in mammalian development and cancer. *Nat. Rev. Mol. Cell Biol.*, **22**, 326–345.
15. Cao,R., Wang,L., Wang,H., Xia,L., Erdjument-Bromage,H., Tempst,P., Jones,R.S. and Zhang,Y. (2002) Role of histone H3 lysine 27 methylation in Polycomb-group silencing. *Science*, **298**, 1039–1043.
16. Czermin,B., Melfi,R., McCabe,D., Seitz,V., Imhof,A. and Pirrotta,V. (2002) Drosophila enhancer of Zeste/ESC complexes have a histone H3 methyltransferase activity that marks chromosomal Polycomb sites. *Cell*, **111**, 185–196.
17. Kuzmichev,A., Nishioka,K., Erdjument-Bromage,H., Tempst,P. and Reinberg,D. (2002) Histone methyltransferase activity associated with a human multiprotein complex containing the Enhancer of Zeste protein. *Genes Dev.*, **16**, 2893–2905.
18. Muller,J., Hart,C.M., Francis,N.J., Vargas,M.L., Sengupta,A., Wild,B., Miller,E.L., O'Connor,M.B., Kingston,R.E. and Simon,J.A. (2002) Histone methyltransferase activity of a Drosophila Polycomb group repressor complex. *Cell*, **111**, 197–208.
19. Shen,X., Liu,Y., Hsu,Y.J., Fujiwara,Y., Kim,J., Mao,X., Yuan,G.C. and Orkin,S.H. (2008) EZH1 mediates methylation on histone H3 lysine 27 and complements EZH2 in maintaining stem cell identity and executing pluripotency. *Mol. Cell*, **32**, 491–502.
20. Wang,L., Brown,J.L., Cao,R., Zhang,Y., Kassis,J.A. and Jones,R.S. (2004) Hierarchical recruitment of polycomb group silencing complexes. *Mol. Cell*, **14**, 637–646.
21. Wang,H., Wang,L., Erdjument-Bromage,H., Vidal,M., Tempst,P., Jones,R.S. and Zhang,Y. (2004) Role of histone H2A ubiquitination in Polycomb silencing. *Nature*, **431**, 873–878.
22. de Napoles,M., Mermoud,J.E., Wakao,R., Tang,Y.A., Endoh,M., Appanah,R., Nesterova,T.B., Silva,J., Otte,A.P., Vidal,M. *et al.* (2004) Polycomb group proteins Ring1A/B link ubiquitylation of histone H2A to heritable gene silencing and X inactivation. *Dev. Cell*, **7**, 663–676.
23. Blackledge,N.P., Farcas,A.M., Kondo,T., King,H.W., McGouran,J.F., Hanssen,L.L., Ito,S., Cooper,S., Kondo,K., Koseki,Y. *et al.* (2014) Variant PRC1 complex-dependent H2A ubiquitylation drives PRC2 recruitment and polycomb domain formation. *Cell*, **157**, 1445–1459.
24. Cooper,S., Dienstbier,M., Hassan,R., Schermelleh,L., Sharif,J., Blackledge,N.P., De Marco,V., Elderkin,S., Koseki,H., Klose,R. *et al.* (2014) Targeting polycomb to pericentric heterochromatin in embryonic stem cells reveals a role for H2AK119u1 in PRC2 recruitment. *Cell Rep.*, **7**, 1456–1470.
25. Kalb,R., Latwiel,S., Baymaz,H.I., Jansen,P.W., Muller,C.W., Vermeulen,M. and Muller,J. (2014) Histone H2A monoubiquitination promotes histone H3 methylation in Polycomb repression. *Nat. Struct. Mol. Biol.*, **21**, 569–571.
26. Eskeland,R., Leeb,M., Grimes,G.R., Kress,C., Boyle,S., Sproul,D., Gilbert,N., Fan,Y., Skoultchi,A.I., Wutz,A. *et al.* (2010) Ring1B compacts chromatin structure and represses gene expression independent of histone ubiquitination. *Mol. Cell*, **38**, 452–464.
27. Isono,K., Endo,T.A., Ku,M., Yamada,D., Suzuki,R., Sharif,J., Ishikura,T., Toyoda,T., Bernstein,B.E. and Koseki,H. (2013) SAM domain polymerization links subnuclear clustering of PRC1 to gene silencing. *Dev. Cell*, **26**, 565–577.
28. Joshi,O., Wang,S.Y., Kuznetsova,T., Atlasi,Y., Peng,T., Fabre,P.J., Habibi,E., Shaik,J., Saeed,S., Handoko,L. *et al.* (2015) Dynamic reorganization of extremely long-range promoter-promoter interactions between two states of pluripotency. *Cell Stem Cell*, **17**, 748–757.
29. Schoenfelder,S., Sugar,R., Dimond,A., Javierre,B.M., Armstrong,H., Mifsud,B., Dimitrova,E., Matheson,L., Tavares-Cadete,F., Furlan-Magaril,M. *et al.* (2015) Polycomb repressive complex PRC1 spatially constrains the mouse embryonic stem cell genome. *Nat. Genet.*, **47**, 1179–1186.
30. Kundu,S., Ji,F., Sunwoo,H., Jain,G., Lee,J.T., Sadreyev,R.I., Dekker,J. and Kingston,R.E. (2017) Polycomb repressive complex 1 generates discrete compacted domains that change during differentiation. *Mol. Cell*, **65**, 432–446.
31. Boyle,S., Flyamer,I.M., Williamson,I., Sengupta,D., Bickmore,W.A. and Illingworth,R.S. (2020) A central role for canonical PRC1 in shaping the 3D nuclear landscape. *Genes Dev.*, **34**, 931–949.
32. Tatavosian,R., Kent,S., Brown,K., Yao,T., Duc,H.N., Huynh,T.N., Zhen,C.Y., Ma,B., Wang,H. and Ren,X. (2019) Nuclear condensates of the Polycomb protein chromobox 2 (CBX2) assemble through phase separation. *J. Biol. Chem.*, **294**, 1451–1463.
33. Plys,A.J., Davis,C.P., Kim,J., Rizki,G., Keenen,M.M., Marr,S.K. and Kingston,R.E. (2019) Phase separation of Polycomb-repressive complex 1 is governed by a charged disordered region of CBX2. *Genes Dev.*, **33**, 799–813.
34. Kent,S., Brown,K., Yang,C.H., Alsaihati,N., Tian,C., Wang,H. and Ren,X. (2020) Phase-separated transcriptional condensates accelerate target-search process revealed by live-cell single-molecule imaging. *Cell Rep.*, **33**, 108248.
35. Seif,E., Kang,J.J., Sasseville,C., Senkovich,O., Kaltashov,A., Boulier,E.L., Kapur,I., Kim,C.A. and Francis,N.J. (2020) Phase separation by the polyhomeotic sterile alpha motif compartmentalizes Polycomb Group proteins and enhances their activity. *Nat. Commun.*, **11**, 5609.
36. Pirrotta,V. and Li,H.B. (2012) A view of nuclear Polycomb bodies. *Curr. Opin. Genet. Dev.*, **22**, 101–109.
37. Kondo,T., Isono,K., Kondo,K., Endo,T.A., Itohara,S., Vidal,M. and Koseki,H. (2014) Polycomb potentiates meis2 activation in midbrain by mediating interaction of the promoter with a tissue-specific enhancer. *Dev. Cell*, **28**, 94–101.
38. Wani,A.H., Boettiger,A.N., Schorderet,P., Ergun,A., Munger,C., Sadreyev,R.I., Zhuang,X., Kingston,R.E. and Francis,N.J. (2016) Chromatin topology is coupled to Polycomb group protein subnuclear organization. *Nat. Commun.*, **7**, 10291.
39. Grimaud,C., Bantignies,F., Pal-Bhadra,M., Ghana,P., Bhadra,U. and Cavalli,G. (2006) RNAi components are required for nuclear clustering of Polycomb group response elements. *Cell*, **124**, 957–971.
40. Cheutin,T. and Cavalli,G. (2012) Progressive polycomb assembly on H3K27me3 compartments generates polycomb bodies with developmentally regulated motion. *PLos Genet.*, **8**, e1002465.
41. Gonzalez,I., Mateos-Langerak,J., Thomas,A., Cheutin,T. and Cavalli,G. (2014) Identification of regulators of the three-dimensional polycomb organization by a microscopy-based genome-wide RNAi screen. *Mol. Cell*, **54**, 485–499.
42. Schmiedeberg,L., Skene,P., Deaton,A. and Bird,A. (2009) A temporal threshold for formaldehyde crosslinking and fixation. *PLoS One*, **4**, e4636.

43. Teves,S.S., An,L., Hansen,A.S., Xie,L., Darzacq,X. and Tjian,R. (2016) A dynamic mode of mitotic bookmarking by transcription factors. *Elife*, **5**, e22280.

44. Tatavosian,R., Duc,H.N., Huynh,T.N., Fang,D., Schmitt,B., Shi,X., Deng,Y., Phiel,C., Yao,T., Zhang,Z. *et al.* (2018) Live-cell single-molecule dynamics of PcG proteins imposed by the DIPG H3.3K27M mutation. *Nat. Commun.*, **9**, 2080.

45. Zhen,C.Y., Tatavosian,R., Huynh,T.N., Duc,H.N., Das,R., Kokotovic,M., Grimm,J.B., Lavis,L.D., Lee,J., Mejia,F.J. *et al.* (2016) Live-cell single-molecule tracking reveals co-recognition of H3K27me3 and DNA targets polycomb Cbx7-PRC1 to chromatin. *Elife*, **5**, e17667.

46. Chen,J., Zhang,Z., Li,L., Chen,B.C., Revyakin,A., Hajj,B., Legant,W., Dahan,M., Lionnet,T., Betzig,E. *et al.* (2014) Single-molecule dynamics of enhanceosome assembly in embryonic stem cells. *Cell*, **156**, 1274–1285.

47. Swinstead,E.E., Miranda,T.B., Paakinaho,V., Baek,S., Goldstein,I., Hawkins,M., Karpova,T.S., Ball,D., Mazza,D., Lavis,L.D. *et al.* (2016) Steroid receptors reprogram foxa1 occupancy through dynamic chromatin transitions. *Cell*, **165**, 593–605.

48. Mazza,D., Abernathy,A., Golob,N., Morisaki,T. and McNally,J.G. (2012) A benchmark for chromatin binding measurements in live cells. *Nucleic Acids Res.*, **40**, e119.

49. Loffreda,A., Jacchetti,E., Antunes,S., Rainone,P., Daniele,T., Morisaki,T., Bianchi,M.E., Tacchetti,C. and Mazza,D. (2017) Live-cell p53 single-molecule binding is modulated by C-terminal acetylation and correlates with transcriptional activity. *Nat. Commun.*, **8**, 313.

50. Paakinaho,V., Presman,D.M., Ball,D.A., Johnson,T.A., Schiltz,R.L., Levitt,P., Mazza,D., Morisaki,T., Karpova,T.S. and Hager,G.L. (2017) Single-molecule analysis of steroid receptor and cofactor action in living cells. *Nat. Commun.*, **8**, 15896.

51. Gebhardt,J.C., Suter,D.M., Roy,R., Zhao,Z.W., Chapman,A.R., Basu,S., Maniatis,T. and Xie,X.S. (2013) Single-molecule imaging of transcription factor binding to DNA in live mammalian cells. *Nat. Methods*, **10**, 421–426.

52. Normanno,D., Boudarene,L., Dugast-Darzacq,C., Chen,J., Richter,C., Proux,F., Benichou,O., Voituriez,R., Darzacq,X. and Dahan,M. (2015) Probing the target search of DNA-binding proteins in mammalian cells using TetR as model searcher. *Nat. Commun.*, **6**, 7357.

53. Mir,M., Reimer,A., Haines,J.E., Li,X.Y., Stadler,M., Garcia,H., Eisen,M.B. and Darzacq,X. (2017) Dense Bicoid hubs accentuate binding along the morphogen gradient. *Genes Dev.*, **31**, 1784–1794.

54. Morisaki,T., Muller,W.G., Golob,N., Mazza,D. and McNally,J.G. (2014) Single-molecule analysis of transcription factor binding at transcription sites in live cells. *Nat. Commun.*, **5**, 4456.

55. Liu,Z., Lavis,L.D. and Betzig,E. (2015) Imaging live-cell dynamics and structure at the single-molecule level. *Mol. Cell*, **58**, 644–659.

56. Presman,D.M., Ball,D.A., Paakinaho,V., Grimm,J.B., Lavis,L.D., Karpova,T.S. and Hager,G.L. (2017) Quantifying transcription factor binding dynamics at the single-molecule level in live cells. *Methods*, **123**, 76–88.

57. Liu,Z. and Tjian,R. (2018) Visualizing transcription factor dynamics in living cells. *J. Cell Biol.*, **217**, 1181–1191.

58. Elf,J. and Barkefors,I. (2019) Single-molecule kinetics in living cells. *Annu. Rev. Biochem.*, **88**, 635–659.

59. Shukron,O., Seeber,A., Amitai,A. and Holcman,D. (2019) Advances using single-particle trajectories to reconstruct chromatin organization and dynamics. *Trends Genet.*, **35**, 685–705.

60. Agbleke,A.A., Amitai,A., Buenrostro,J.D., Chakrabarti,A., Chu,L., Hansen,A.S., Koenig,K.M., Labade,A.S., Liu,S., Nozaki,T. *et al.* (2020) Advances in chromatin and chromosome research: perspectives from multiple fields. *Mol. Cell*, **79**, 881–901.

61. Laugesen,A., Hojfeldt,J.W. and Helin,K. (2019) Molecular mechanisms directing PRC2 recruitment and H3K27 methylation. *Mol. Cell*, **74**, 8–18.

62. Yu,J.R., Lee,C.H., Oksuz,O., Stafford,J.M. and Reinberg,D. (2019) PRC2 is high maintenance. *Gene Dev*, **33**, 903–935.

63. Margueron,R., Li,G., Sarma,K., Blais,A., Zavadil,J., Woodcock,C.L., Dynlacht,B.D. and Reinberg,D. (2008) Ezh1 and Ezh2 maintain repressive chromatin through different mechanisms. *Mol. Cell*, **32**, 503–518.

64. Margueron,R., Justin,N., Ohno,K., Sharpe,M.L., Son,J., Drury,W.J. 3rd, Voigt,P., Martin,S.R., Taylor,W.R., De Marco,V. *et al.* (2009) Role of the polycomb protein EED in the propagation of repressive histone marks. *Nature*, **461**, 762–767.

65. Xu,C., Bian,C., Yang,W., Galka,M., Ouyang,H., Chen,C., Qiu,W., Liu,H., Jones,A.E., MacKenzie,F. *et al.* (2010) Binding of different histone marks differentially regulates the activity and specificity of polycomb repressive complex 2 (PRC2). *Proc. Natl. Acad. Sci. U.S.A.*, **107**, 19266–19271.

66. Hojfeldt,J.W., Laugesen,A., Willumsen,B.M., Damhofer,H., Hedehus,L., Tvardovskiy,A., Mohammad,F., Jensen,O.N. and Helin,K. (2018) Accurate H3K27 methylation can be established de novo by SUZ12-directed PRC2. *Nat. Struct. Mol. Biol.*, **25**, 225–232.

67. Youmans,D.T., Schmidt,J.C. and Cech,T.R. (2018) Live-cell imaging reveals the dynamics of PRC2 and recruitment to chromatin by SUZ12-associated subunits. *Genes Dev.*, **32**, 794–805.

68. Youmans,D.T., Gooding,A.R., Dowell,R.D. and Cech,T.R. (2021) Competition between PRC2.1 and 2.2 subcomplexes regulates PRC2 chromatin occupancy in human stem cells. *Mol. Cell*, **81**, 488–501.

69. Schmitges,F.W., Prusty,A.B., Faty,M., Stutzer,A., Lingaraju,G.M., Aiwazian,J., Sack,R., Hess,D., Li,L., Zhou,S. *et al.* (2011) Histone methylation by PRC2 is inhibited by active chromatin marks. *Mol. Cell*, **42**, 330–341.

70. Beringer,M., Pisano,P., Di Carlo,V., Blanco,E., Chammas,P., Vizan,P., Gutierrez,A., Aranda,S., Payer,B., Wierer,M. *et al.* (2016) EPOP functionally links elongin and Polycomb in pluripotent stem cells. *Mol. Cell*, **64**, 645–658.

71. Conway,E., Jerman,E., Healy,E., Ito,S., Holoch,D., Oliviero,G., Deevy,O., Glancy,E., Fitzpatrick,D.J., Mucha,M. *et al.* (2018) A family of vertebrate-specific Polycombs encoded by the LCOR/LCORL genes balance PRC2 subtype activities. *Mol. Cell*, **70**, 408–421.

72. Liefke,R., Karwacki-Neisius,V. and Shi,Y. (2016) EPOP interacts with elongin BC and USP7 to modulate the chromatin landscape. *Mol. Cell*, **64**, 659–672.

73. Ballare,C., Lange,M., Lapinaite,A., Martin,G.M., Morey,L., Pascual,G., Liefke,R., Simon,B., Shi,Y., Gozani,O. *et al.* (2012) Phf19 links methylated Lys36 of histone H3 to regulation of Polycomb activity. *Nat. Struct. Mol. Biol.*, **19**, 1257–1265.

74. Brien,G.L., Gambero,G., O'Connell,D.J., Jerman,E., Turner,S.A., Egan,C.M., Dunne,E.J., Jurgens,M.C., Wynne,K., Piao,L. *et al.* (2012) Polycomb PHF19 binds H3K36me3 and recruits PRC2 and demethylase NO66 to embryonic stem cell genes during differentiation. *Nat. Struct. Mol. Biol.*, **19**, 1273–1281.

75. Musselman,C.A., Avvakumov,N., Watanabe,R., Abraham,C.G., Lalonde,M.E., Hong,Z., Allen,C., Roy,S., Nunez,J.K., Nickoloff,J. *et al.* (2012) Molecular basis for H3K36me3 recognition by the Tudor domain of PHF1. *Nat. Struct. Mol. Biol.*, **19**, 1266–1272.

76. Cai,L., Rothbart,S.B., Lu,R., Xu,B., Chen,W.Y., Tripathy,A., Rockowitz,S., Zheng,D., Patel,D.J., Allis,C.D. *et al.* (2013) An H3K36 methylation-engaging Tudor motif of polycomb-like proteins mediates PRC2 complex targeting. *Mol. Cell*, **49**, 571–582.

77. Li,H., Liefke,R., Jiang,J., Kurland,J.V., Tian,W., Deng,P., Zhang,W., He,Q., Patel,D.J., Bulyk,M.L. *et al.* (2017) Polycomb-like proteins link the PRC2 complex to CpG islands. *Nature*, **549**, 287–291.

78. Perino,M., van Mierlo,G., Karemaker,I.D., van Genesen,S., Vermeulen,M., Marks,H., van Heeringen,S.J. and Veenstra,G.J.C. (2018) MTF2 recruits Polycomb Repressive Complex 2 by helical-shape-selective DNA binding. *Nat. Genet.*, **50**, 1002–1010.

79. Zhang,Z., Jones,A., Sun,C.W., Li,C., Chang,C.W., Joo,H.Y., Dai,Q., Mysliwiec,M.R., Wu,L.C., Guo,Y. *et al.* (2011) PRC2 complexes with JARID2, MTF2, and esPRC2p48 in ES cells to modulate ES cell pluripotency and somatic cell reprogramming. *Stem Cells*, **29**, 229–240.

80. Kim,H., Kang,K. and Kim,J. (2009) AEBP2 as a potential targeting protein for Polycomb Repression Complex PRC2. *Nucleic. Acids. Res.*, **37**, 2940–2950.

81. Peng,J.C., Valouev,A., Swigut,T., Zhang,J., Zhao,Y., Sidow,A. and Wysocka,J. (2009) Jarid2/Jumonji coordinates control of PRC2 enzymatic activity and target gene occupancy in pluripotent cells. *Cell*, **139**, 1290–1302.

82. Shen,X., Kim,W., Fujiwara,Y., Simon,M.D., Liu,Y., Mysliwiec,M.R., Yuan,G.C., Lee,Y. and Orkin,S.H. (2009) Jumonji

modulates polycomb activity and self-renewal versus differentiation of stem cells. *Cell*, **139**, 1303–1314.

83. Cooper,S., Grijzenhout,A., Underwood,E., Ancelin,K., Zhang,T., Nesterova,T.B., Anil-Kirmizitas,B., Bassett,A., Kooistra,S.M., Agger,K. *et al.* (2016) Jarid2 binds mono-ubiquitylated H2A lysine 119 to mediate crosstalk between Polycomb complexes PRC1 and PRC2. *Nat. Commun.*, **7**, 13661.

84. Lee,C.H., Holder,M., Grau,D., Saldana-Meyer,R., Yu,J.R., Ganai,R.A., Zhang,J., Wang,M., LeRoy,G., Dobenecker,M.W. *et al.* (2018) Distinct stimulatory mechanisms regulate the catalytic activity of Polycomb Repressive Complex 2. *Mol. Cell*, **70**, 435–448.

85. Hojfeldt,J.W., Hedehus,L., Laugesen,A., Tatar,T., Wiehle,L. and Helin,K. (2019) Non-core subunits of the PRC2 complex are collectively required for its target-site specificity. *Mol. Cell*, **76**, 423–436.

86. Healy,E., Mucha,M., Glancy,E., Fitzpatrick,D.J., Conway,E., Neikes,H.K., Monger,C., Van Mierlo,G., Baltissen,M.P., Koseki,Y. *et al.* (2019) PRC2.1 and PRC2.2 synergize to coordinate H3K27 trimethylation. *Mol. Cell*, **76**, 437–452.

87. Gao,Z., Zhang,J., Bonasio,R., Strino,F., Sawai,A., Parisi,F., Kluger,Y. and Reinberg,D. (2012) PCGF homologs, CBX proteins, and RYBP define functionally distinct PRC1 family complexes. *Mol. Cell*, **45**, 344–356.

88. Tavares,L., Dimitrova,E., Oxley,D., Webster,J., Poot,R., Demmers,J., Bezstarosti,K., Taylor,S., Ura,H., Koide,H. *et al.* (2012) RYBP-PRC1 complexes mediate H2A ubiquitination at polycomb target sites independently of PRC2 and H3K27me3. *Cell*, **148**, 664–678.

89. Hauri,S., Comoglio,F., Seimiya,M., Gerstung,M., Glatter,T., Hansen,K., Aebersold,R., Paro,R., Gstaiger,M. and Beisel,C. (2016) A high-density map for navigating the human Polycomb complexome. *Cell Rep.*, **17**, 583–595.

90. Kloet,S.L., Makowski,M.M., Baymaz,H.I., van Voorthuijsen,L., Karemaker,I.D., Santanach,A., Jansen,P., Di Croce,L. and Vermeulen,M. (2016) The dynamic interactome and genomic targets of Polycomb complexes during stem-cell differentiation. *Nat. Struct. Mol. Biol.*, **23**, 682–690.

91. Kaustov,L., Ouyang,H., Amaya,M., Lemak,A., Nady,N., Duan,S., Wasney,G.A., Li,Z., Vedadi,M., Schapira,M. *et al.* (2011) Recognition and specificity determinants of the human cbx chromodomains. *J. Biol. Chem.*, **286**, 521–529.

92. Bernstein,E., Duncan,E.M., Masui,O., Gil,J., Heard,E. and Allis,C.D. (2006) Mouse polycomb proteins bind differentially to methylated histone H3 and RNA and are enriched in facultative heterochromatin. *Mol. Cell. Biol.*, **26**, 2560–2569.

93. Tardat,M., Albert,M., Kunzmann,R., Liu,Z., Kaustov,L., Thierry,R., Duan,S., Brykczynska,U., Arrowsmith,C.H. and Peters,A.H. (2015) Cbx2 targets PRC1 to constitutive heterochromatin in mouse zygotes in a parent-of-origin-dependent manner. *Mol. Cell*, **58**, 157–171.

94. Kim,C.A., Gingery,M., Pilpa,R.M. and Bowie,J.U. (2002) The SAM domain of polyhomeotic forms a helical polymer. *Nat. Struct. Biol.*, **9**, 453–457.

95. Grau,D.J., Chapman,B.A., Garlick,J.D., Borowsky,M., Francis,N.J. and Kingston,R.E. (2011) Compaction of chromatin by diverse Polycomb group proteins requires localized regions of high charge. *Genes Dev.*, **25**, 2210–2221.

96. Lau,M.S., Schwartz,M.G., Kundu,S., Savol,A.J., Wang,P.I., Marr,S.K., Grau,D.J., Schorderet,P., Sadreyev,R.I., Tabin,C.J. *et al.* (2017) Mutation of a nucleosome compaction region disrupts Polycomb-mediated axial patterning. *Science*, **355**, 1081–1084.

97. Morey,L., Pascual,G., Cozzuto,L., Roma,G., Wutz,A., Benitah,S.A. and Di Croce,L. (2012) Nonoverlapping functions of the Polycomb group Cbx family of proteins in embryonic stem cells. *Cell Stem Cell*, **10**, 47–62.

98. Wang,R.J., Taylor,A.B., Leal,B.Z., Chadwell,L.V., Ilangovan,U., Robinson,A.K., Schirf,V., Hart,P.J., Lafer,E.M., Demeler,B. *et al.* (2010) Polycomb group targeting through Different Binding Partners of RING1B C-Terminal Domain. *Structure*, **18**, 966–975.

99. Rose,N.R., King,H.W., Blackledge,N.P., Fursova,N.A., Ember,K.J., Fischer,R., Kessler,B.M. and Klose,R.J. (2016) RYBP stimulates PRC1 to shape chromatin-based communication between Polycomb repressive complexes. *Elife*, **5**, e18591.

100. Scelfo,A., Fernandez-Perez,D., Tamburri,S., Zanotti,M., Lavarone,E., Soldi,M., Bonaldi,T., Ferrari,K.J. and Pasini,D. (2019) Functional landscape of PCGF proteins reveals both RING1A/B-dependent-and RING1A/B-independent-specific activities. *Mol. Cell*, **74**, 1037–1052.

101. Fursova,N.A., Blackledge,N.P., Nakayama,M., Ito,S., Koseki,Y., Farcas,A.M., King,H.W., Koseki,H. and Klose,R.J. (2019) Synergy between variant PRC1 complexes defines Polycomb-mediated gene repression. *Mol. Cell*, **74**, 1020–1036.

102. Zhao,J., Wang,M., Chang,L., Yu,J., Song,A., Liu,C., Huang,W., Zhang,T., Wu,X., Shen,X. *et al.* (2020) RYBP/YAF2-PRC1 complexes and histone H1-dependent chromatin compaction mediate propagation of H2AK119ub1 during cell division. *Nat. Cell Biol.*, **22**, 439–452.

103. Farcas,A.M., Blackledge,N.P., Sudbery,I., Long,H.K., McGouran,J.F., Rose,N.R., Lee,S., Sims,D., Cerase,A., Sheahan,T.W. *et al.* (2012) KDM2B links the Polycomb Repressive Complex 1 (PRC1) to recognition of CpG islands. *Elife*, **1**, e00205.

104. He,J., Shen,L., Wan,M., Taranova,O., Wu,H. and Zhang,Y. (2013) Kdm2b maintains murine embryonic stem cell status by recruiting PRC1 complex to CpG islands of developmental genes. *Nat. Cell Biol.*, **15**, 373–384.

105. Wu,X., Johansen,J.V. and Helin,K. (2013) Fbxl10/Kdm2b recruits polycomb repressive complex 1 to CpG islands and regulates H2A ubiquitylation. *Mol. Cell*, **49**, 1134–1146.

106. Endoh,M., Endo,T.A., Shinga,J., Hayashi,K., Farcas,A., Ma,K.W., Ito,S., Sharif,J., Endoh,T., Onaga,N. *et al.* (2017) PCGF6-PRC1 suppresses premature differentiation of mouse embryonic stem cells by regulating germ cell-related genes. *Elife*, **6**, e21064.

107. Stielow,B., Finkernagel,F., Stiewe,T., Nist,A. and Suske,G. (2018) MGA, L3MBTL2 and E2F6 determine genomic binding of the non-canonical Polycomb repressive complex PRC1.6. *PLoS Genet.*, **14**, e1007193.

108. Blackledge,N.P., Fursova,N.A., Kelley,J.R., Huseyin,M.K., Feldmann,A. and Klose,R.J. (2020) PRC1 catalytic activity is central to Polycomb system function. *Mol. Cell*, **77**, 857–874.

109. Tamburri,S., Lavarone,E., Fernandez-Perez,D., Conway,E., Zanotti,M., Manganaro,D. and Pasini,D. (2020) Histone H2AK119 mono-ubiquitination is essential for Polycomb-mediated transcriptional repression. *Mol. Cell*, **77**, 840–856.

110. Izeddin,I., Recamier,V., Bosanac,L., Cisse,I.I., Boudarene,L., Dugast-Darzacq,C., Proux,F., Benichou,O., Voituriez,R., Bensaude,O. *et al.* (2014) Single-molecule tracking in live cells reveals distinct target-search strategies of transcription factors in the nucleus. *Elife*, **3**, e02230.

111. Grimm,J.B., English,B.P., Chen,J., Slaughter,J.P., Zhang,Z., Revyakin,A., Patel,R., Macklin,J.J., Normanno,D., Singer,R.H. *et al.* (2015) A general method to improve fluorophores for live-cell and single-molecule microscopy. *Nat. Methods*, **12**, 244–250.

112. Grimm,J.B., English,B.P., Choi,H., Muthusamy,A.K., Mehl,B.P., Dong,P., Brown,T.A., Lippincott-Schwartz,J., Liu,Z., Lionnet,T. *et al.* (2016) Bright photoactivatable fluorophores for single-molecule imaging. *Nat. Methods*, **13**, 985–988.

113. Hansen,A.S., Pustova,I., Cattoglio,C., Tjian,R. and Darzacq,X. (2017) CTCF and cohesin regulate chromatin loop stability with distinct dynamics. *Elife*, **6**, e25776.

114. Cong,L., Ran,F.A., Cox,D., Lin,S., Barretto,R., Habib,N., Hsu,P.D., Wu,X., Jiang,W., Marraffini,L.A. *et al.* (2013) Multiplex genome engineering using CRISPR/Cas systems. *Science*, **339**, 819–823.

115. Jinek,M., East,A., Cheng,A., Lin,S., Ma,E. and Doudna,J. (2013) RNA-programmed genome editing in human cells. *Elife*, **2**, e00471.

116. Tokunaga,M., Imamoto,N. and Sakata-Sogawa,K. (2008) Highly inclined thin illumination enables clear single-molecule imaging in cells. *Nat. Methods*, **5**, 159–161.

117. Verveer,P.J., Swoger,J., Pampaloni,F., Greger,K., Marcello,M. and Stelzer,E.H. (2007) High-resolution three-dimensional imaging of large specimens with light sheet-based microscopy. *Nat. Methods*, **4**, 311–313.

118. Chen,B.C., Legant,W.R., Wang,K., Shao,L., Milkie,D.E., Davidson,M.W., Janetopoulos,C., Wu,X.F.S., Hammer,J.A., Liu,Z. *et al.* (2014) Lattice light-sheet microscopy: Imaging molecules to embryos at high spatiotemporal resolution. *Science*, **346**, 1257998.

119. Abrahamsson,S., Chen,J., Hajj,B., Stallinga,S., Katsov,A.Y., Wisniewski,J., Mizuguchi,G., Soule,P., Mueller,F., Dugast

Darzacq,C. *et al.* (2013) Fast multicolor 3D imaging using aberration-corrected multifocus microscopy. *Nat. Methods*, **10**, 60–63.

120. Hansen,A.S., Amitai,A., Cattoglio,C., Tjian,R. and Darzacq,X. (2020) Guided nuclear exploration increases CTCF target search efficiency. *Nat. Chem. Biol.*, **16**, 257–266.

121. Garcia,D.A., Fettweis,G., Presman,D.M., Paakinaho,V., Jarzynski,C., Upadhyaya,A. and Hager,G.L. (2021) Power-law behavior of transcription factor dynamics at the single-molecule level implies a continuum affinity model. *Nucleic Acids Res.*, doi:10.1093/nar/gkab072.

122. Garcia,D.A., Johnson,T.A., Presman,D.M., Fettweis,G., Wagh,K., Rinaldi,L., Stavreva,D.A., Paakinaho,V., Jensen,R.A.M., Mandrup,S. *et al.* (2021) An intrinsically disordered region-mediated confinement state contributes to the dynamics and function of transcription factors. *Mol. Cell*, **81**, 1484–1498.

123. Hansen,A.S., Woringer,M., Grimm,J.B., Lavis,L.D., Tjian,R. and Darzacq,X. (2018) Robust model-based analysis of single-particle tracking experiments with Spot-On. *Elife*, **7**, e33125.

124. Serge,A., Bertaux,N., Rigneault,H. and Marguet,D. (2008) Dynamic multiple-target tracing to probe spatiotemporal cartography of cell membranes. *Nat. Methods*, **5**, 687–694.

125. Jaqaman,K., Loerke,D., Mettlen,M., Kuwata,H., Grinstein,S., Schmid,S.L. and Danuser,G. (2008) Robust single-particle tracking in live-cell time-lapse sequences. *Nat. Methods*, **5**, 695–702.

126. Mazza,D., Ganguly,S. and McNally,J.G. (2013) Monitoring dynamic binding of chromatin proteins in vivo by single-molecule tracking. *Methods Mol. Biol.*, **1042**, 117–137.

127. Ranjan,A., Nguyen,V.Q., Liu,S., Wisniewski,J., Kim,J.M., Tang,X., Mizuguchi,G., Elalaoui,E., Nickels,T.J., Jou,V. *et al.* (2020) Live-cell single particle imaging reveals the role of RNA polymerase II in histone H2A.Z eviction. *Elife*, **9**, e55667.

128. Watanabe,N. and Mitchison,T.J. (2002) Single-molecule speckle analysis of actin filament turnover in lamellipodia. *Science*, **295**, 1083–1086.

129. Elf,J., Li,G.W. and Xie,X.S. (2007) Probing transcription factor dynamics at the single-molecule level in a living cell. *Science*, **316**, 1191–1194.

130. Liu,H., Dong,P., Ioannou,M.S., Li,L., Shea,J., Pasolli,H.A., Grimm,J.B., Rivlin,P.K., Lavis,L.D., Koyama,M. *et al.* (2018) Visualizing long-term single-molecule dynamics in vivo by stochastic protein labeling. *Proc. Natl. Acad. Sci. U.S.A.*, **115**, 343–348.

131. Hipp,L., Beer,J., Kuchler,O., Reisser,M., Sinske,D., Michaelis,J., Gebhardt,J.C.M. and Knoll,B. (2019) Single-molecule imaging of the transcription factor SRF reveals prolonged chromatin-binding kinetics upon cell stimulation. *Proc. Natl. Acad. Sci. U.S.A.*, **116**, 880–889.

132. Ruthenburg,A.J., Li,H., Patel,D.J. and Allis,C.D. (2007) Multivalent engagement of chromatin modifications by linked binding modules. *Nat. Rev. Mol. Cell Biol.*, **8**, 983–994.

133. Lalonde,M.E., Cheng,X. and Cote,J. (2014) Histone target selection within chromatin: an exemplary case of teamwork. *Genes Dev.*, **28**, 1029–1041.

134. Rando,O.J. (2012) Combinatorial complexity in chromatin structure and function: revisiting the histone code. *Curr. Opin. Genet. Dev.*, **22**, 148–155.

135. Huseyin,M.K. and Klose,R.J. (2021) Live-cell single particle tracking of PRC1 reveals a highly dynamic system with low target site occupancy. *Nat. Commun.*, **12**, 887.

136. Ku,M., Koche,R.P., Rheinbay,E., Mendenhall,E.M., Endoh,M., Mikkelsen,T.S., Presser,A., Nusbaum,C., Xie,X., Chi,A.S. *et al.* (2008) Genomewide analysis of PRC1 and PRC2 occupancy identifies two classes of bivalent domains. *PLoS Genet.*, **4**, e1000242.

137. Jiao,L. and Liu,X. (2015) Structural basis of histone H3K27 trimethylation by an active polycomb repressive complex 2. *Science*, **350**, aac4383.

138. Kawaguchi,T., Machida,S., Kurumizaka,H., Tagami,H. and Nakayama,J.I. (2017) Phosphorylation of CBX2 controls its nucleosome-binding specificity. *J. Biochem.*, **162**, 343–355.

139. Henninger,J.E., Oksuz,O., Shrinivas,K., Sagi,I., LeRoy,G., Zheng,M.M., Andrews,J.O., Zamudio,A.V., Lazaris,C., Hannett,N.M. *et al.* (2021) RNA-mediated feedback control of transcriptional condensates. *Cell*, **184**, 207–225.

140. Zhen,C.Y., Duc,H.N., Kokotovic,M., Phiel,C.J. and Ren,X. (2014) Cbx2 stably associates with mitotic chromosomes via a PRC2- or PRC1-independent mechanism and is needed for recruiting PRC1 complex to mitotic chromosomes. *Mol. Biol. Cell*, **25**, 3726–3739.

141. Baumann,C., Zhang,X. and De La Fuente,R. (2020) Loss of CBX2 induces genome instability and senescence-associated chromosomal rearrangements. *J. Cell Biol.*, **219**, e201910149.

142. Gearhart,M.D., Corcoran,C.M., Wamstad,J.A. and Bardwell,V.J. (2006) Polycomb group and SCF ubiquitin ligases are found in a novel BCOR complex that is recruited to BCL6 targets. *Mol. Cell. Biol.*, **26**, 6880–6889.

143. Kasinath,V., Faini,M., Poepsel,S., Reif,D., Feng,X.A., Stjepanovic,G., Aebersold,R. and Nogales,E. (2018) Structures of human PRC2 with its cofactors AEBP2 and JARID2. *Science*, **359**, 940–944.

144. Choi,J., Bachmann,A.L., Tauscher,K., Benda,C., Fierz,B. and Muller,J. (2017) DNA binding by PHF1 prolongs PRC2 residence time on chromatin and thereby promotes H3K27 methylation. *Nat. Struct. Mol. Biol.*, **24**, 1039–1047.

145. Wang,X., Paucek,R.D., Gooding,A.R., Brown,Z.Z., Ge,E.J., Muir,T.W. and Cech,T.R. (2017) Molecular analysis of PRC2 recruitment to DNA in chromatin and its inhibition by RNA. *Nat. Struct. Mol. Biol.*, **24**, 1028–1038.

146. Finogenova,K., Bonnet,J., Poepsel,S., Schafer,I.B., Finkl,K., Schmid,K., Litz,C., Strauss,M., Benda,C. and Muller,J. (2020) Structural basis for PRC2 decoding of active histone methylation marks H3K36me2/3. *Elife*, **9**, e61964.

147. Kasinath,V., Beck,C., Sauer,P., Poepsel,S., Kosmatka,J., Faini,M., Toso,D., Aebersold,R. and Nogales,E. (2021) JARID2 and AEBP2 regulate PRC2 in the presence of H2AK119ub1 and other histone modifications. *Science*, **371**, eabc3393.

148. Cavalli,G. and Heard,E. (2019) Advances in epigenetics link genetics to the environment and disease. *Nature*, **571**, 489–499.

149. Ferrari,K.J., Scelfo,A., Jammula,S., Cuomo,A., Barozzi,I., Stutzer,A., Fischle,W., Bonaldi,T. and Pasini,D. (2014) Polycomb-dependent H3K27me1 and H3K27me2 regulate active transcription and enhancer fidelity. *Mol. Cell*, **53**, 49–62.

150. Jung,H.R., Pasini,D., Helin,K. and Jensen,O.N. (2010) Quantitative mass spectrometry of histones H3.2 and H3.3 in Suz12-deficient mouse embryonic stem cells reveals distinct, dynamic post-translational modifications at Lys-27 and Lys-36. *Mol. Cell. Proteomics*, **9**, 838–850.

151. Tatavosian,R., Zhen,C.Y., Duc,H.N., Balas,M.M., Johnson,A.M. and Ren,X. (2015) Distinct Cellular Assembly Stoichiometry of Polycomb Complexes on Chromatin Revealed by Single-molecule Chromatin Immunoprecipitation Imaging. *J. Biol. Chem.*, **290**, 28033–28054.

152. Riggs,A.D., Bourgeois,S. and Cohn,M. (1970) The lac repressor-operator interaction. 3. Kinetic studies. *J. Mol. Biol.*, **53**, 401–417.

153. von Hippel,P.H. and Berg,O.G. (1989) Facilitated target location in biological systems. *J. Biol. Chem.*, **264**, 675–678.

154. Hammar,P., Leroy,P., Mahmutovic,A., Marklund,E.G., Berg,O.G. and Elf,J. (2012) The lac repressor displays facilitated diffusion in living cells. *Science*, **336**, 1595–1598.

155. McSwiggen,D.T., Mir,M., Darzacq,X. and Tjian,R. (2019) Evaluating phase separation in live cells: diagnosis, caveats, and functional consequences. *Genes Dev.*, **33**, 1619–1634.

156. McSwiggen,D.T., Hansen,A.S., Teves,S.S., Marie-Nelly,H., Hao,Y., Heckert,A.B., Umemoto,K.K., Dugast-Darzacq,C., Tjian,R. and Darzacq,X. (2019) Evidence for DNA-mediated nuclear compartmentalization distinct from phase separation. *Elife*, **8**, e47098.

157. Boija,A., Klein,I.A., Sabari,B.R., Dall'Agnese,A., Coffey,E.L., Zamudio,A.V., Li,C.H., Shrinivas,K., Manteiga,J.C., Hannett,N.M. *et al.* (2018) Transcription factors activate genes through the phase-separation capacity of their activation domains. *Cell*, **175**, 1842–1855.

158. Chong,S., Dugast-Darzacq,C., Liu,Z., Dong,P., Dailey,G.M., Cattoglio,C., Heckert,A., Banala,S., Lavis,L., Darzacq,X. *et al.* (2018) Imaging dynamic and selective low-complexity domain interactions that control gene transcription. *Science*, **361**, eaar2555.

159. Cho,W.K., Spille,J.H., Hecht,M., Lee,C., Li,C., Grube,V. and Cisse,I.I. (2018) Mediator and RNA polymerase II clusters associate in transcription-dependent condensates. *Science*, **361**, 412–415.

160. Sabari,B.R., Dall'Agnese,A., Boija,A., Klein,I.A., Coffey,E.L., Shrinivas,K., Abraham,B.J., Hannett,N.M., Zamudio,A.V., Manteiga,J.C. *et al.* (2018) Coactivator condensation at super-enhancers links phase separation and gene control. *Science*, **361**, eaar3958.

161. Voigt,P., Tee,W.W. and Reinberg,D. (2013) A double take on bivalent promoters. *Genes Dev.*, **27**, 1318–1338.

162. Klose,R.J., Cooper,S., Farcas,A.M., Blackledge,N.P. and Brockdorff,N. (2013) Chromatin sampling–an emerging perspective on targeting polycomb repressor proteins. *PLoS Genet.*, **9**, e1003717.

163. Mao,Y.S., Zhang,B. and Spector,D.L. (2011) Biogenesis and function of nuclear bodies. *Trends Genet.*, **27**, 295–306.

164. Banani,S.F., Lee,H.O., Hyman,A.A. and Rosen,M.K. (2017) Biomolecular condensates: organizers of cellular biochemistry. *Nat. Rev. Mol. Cell Biol.*, **18**, 285–298.

165. Hyman,A.A., Weber,C.A. and Julicher,F. (2014) Liquid-liquid phase separation in biology. *Annu. Rev. Cell Dev. Biol.*, **30**, 39–58.

166. Shin,Y. and Brangwynne,C.P. (2017) Liquid phase condensation in cell physiology and disease. *Science*, **357**, eaaf4382.

167. Stroberg,W. and Schnell,S. (2018) Do cellular condensates accelerate biochemical reactions? Lessons from microdroplet chemistry. *Biophys. J.*, **115**, 3–8.

168. Boehning,M., Dugast-Darzacq,C., Rankovic,M., Hansen,A.S., Yu,T., Marie-Nelly,H., McSwiggen,D.T., Kokic,G., Dailey,G.M., Cramer,P. *et al.* (2018) RNA polymerase II clustering through carboxy-terminal domain phase separation. *Nat. Struct. Mol. Biol.*, **25**, 833–840.

169. Lu,H., Yu,D., Hansen,A.S., Ganguly,S., Liu,R., Heckert,A., Darzacq,X. and Zhou,Q. (2018) Phase-separation mechanism for C-terminal hyperphosphorylation of RNA polymerase II. *Nature*, **558**, 318–323.

170. Shrinivas,K., Sabari,B.R., Coffey,E.L., Klein,I.A., Boija,A., Zamudio,A.V., Schuijers,J., Hannett,N.M., Sharp,P.A., Young,R.A. *et al.* (2019) Enhancer features that drive formation of transcriptional condensates. *Mol. Cell*, **75**, 549–561.

171. Zamudio,A.V., Dall'Agnese,A., Henninger,J.E., Manteiga,J.C., Afeyan,L.K., Hannett,N.M., Coffey,E.L., Li,C.H., Oksuz,O., Sabari,B.R. *et al.* (2019) Mediator condensates localize signaling factors to key cell identity genes. *Mol. Cell*, **76**, 753–766.

172. Guo,Y.E., Manteiga,J.C., Henninger,J.E., Sabari,B.R., Dall'Agnese,A., Hannett,N.M., Spille,J.H., Afeyan,L.K., Zamudio,A.V., Shrinivas,K. *et al.* (2019) Pol II phosphorylation regulates a switch between transcriptional and splicing condensates. *Nature*, **572**, 543–548.

173. Nair,S.J., Yang,L., Meluzzi,D., Oh,S., Yang,F., Friedman,M.J., Wang,S., Suter,T., Alshareedah,I., Gamliel,A. *et al.* (2019) Phase separation of ligand-activated enhancers licenses cooperative chromosomal enhancer assembly. *Nat. Struct. Mol. Biol.*, **26**, 193–203.

174. Gallego,L.D., Schneider,M., Mittal,C., Romanauska,A., Gudino Carrillo,R.M., Schubert,T., Pugh,B.F. and Kohler,A. (2020) Phase separation directs ubiquitination of gene-body nucleosomes. *Nature*, **579**, 592–597.

175. Strom,A.R., Emelyanov,A.V., Mir,M., Fyodorov,D.V., Darzacq,X. and Karpen,G.H. (2017) Phase separation drives heterochromatin domain formation. *Nature*, **547**, 241–245.

176. Larson,A.G., Elnatan,D., Keenen,M.M., Trnka,M.J., Johnston,J.B., Burlingame,A.L., Agard,D.A., Redding,S. and Narlikar,G.J. (2017) Liquid droplet formation by HP1alpha suggests a role for phase separation in heterochromatin. *Nature*, **547**, 236–240.

177. Sanulli,S., Trnka,M.J., Dharmarajan,V., Tibble,R.W., Pascal,B.D., Burlingame,A.L., Griffin,P.R., Gross,J.D. and Narlikar,G.J. (2019) HP1 reshapes nucleosome core to promote phase separation of heterochromatin. *Nature*, **575**, 390–394.

178. Wang,L., Gao,Y., Zheng,X., Liu,C., Dong,S., Li,R., Zhang,G., Wei,Y., Qu,H., Li,Y. *et al.* (2019) Histone modifications regulate chromatin compartmentalization by contributing to a phase separation mechanism. *Mol. Cell*, **76**, 646–659.

179. Erdel,F., Rademacher,A., Vlijm,R., Tunnermann,J., Frank,L., Weinmann,R., Schweigert,E., Yserentant,K., Hummert,J., Bauer,C. *et al.* (2020) Mouse heterochromatin adopts digital compaction states without showing hallmarks of HP1-driven liquid-liquid phase separation. *Mol. Cell*, **78**, 236–249.

180. Gibson,B.A., Doolittle,L.K., Schneider,M.W.G., Jensen,L.E., Gamarra,N., Henry,L., Gerlich,D.W., Redding,S. and Rosen,M.K. (2019) Organization of Chromatin by Intrinsic and Regulated Phase Separation. *Cell*, **179**, 470–484.

181. Hnisz,D., Shrinivas,K., Young,R.A., Chakraborty,A.K. and Sharp,P.A. (2017) A phase separation model for transcriptional control. *Cell*, **169**, 13–23.

182. Klosin,A. and Hyman,A.A. (2017) Molecular biology: a liquid reservoir for silent chromatin. *Nature*, **547**, 168–170.

183. Plys,A.J. and Kingston,R.E. (2018) Dynamic condensates activate transcription. *Science*, **361**, 329–330.

184. Hahn,S. (2018) Phase separation, protein disorder, and enhancer function. *Cell*, **175**, 1723–1725.

185. Falahati,H., Pelham-Webb,B., Blythe,S. and Wieschaus,E. (2016) Nucleation by rRNA dictates the precision of nucleolus assembly. *Curr. Biol.*, **26**, 277–285.

186. Francis,N.J., Kingston,R.E. and Woodcock,C.L. (2004) Chromatin compaction by a polycomb group protein complex. *Science*, **306**, 1574–1577.

187. Ren,X., Vincenz,C. and Kerppola,T.K. (2008) Changes in the distributions and dynamics of polycomb repressive complexes during embryonic stem cell differentiation. *Mol. Cell. Biol.*, **28**, 2884–2895.

188. Chen,S., Jiao,L., Liu,X., Yang,X. and Liu,X. (2020) A dimeric structural scaffold for PRC2-PCL targeting to CpG island chromatin. *Mol. Cell*, **77**, 1265–1278.

189. Poepsel,S., Kasinath,V. and Nogales,E. (2018) Cryo-EM structures of PRC2 simultaneously engaged with two functionally distinct nucleosomes. *Nat. Struct. Mol. Biol.*, **25**, 154–162.